AN ABSTRACT OF THE THESIS OF

Eleas M. Wu for the degree of Master of Science in Comparative Health Sciences presented on June 5, 2019.

Title: Expression of Follicle Stimulating Hormone (FSHβ) and its Receptor (FSHR) within the Ovine Placentome

Abstract approved:

_____

Charles T. Estill

Follicle stimulating hormone (FSH) plays a key role in the ewe's estrous cycle but understanding its continued importance during pregnancy is not well understood. Researchers have proposed a model theorizing that a cascade of hormones is responsible for pregnancy maintenance. Weems et al. proposed a model for placental progesterone production; theorizing progesterone secretion is intricately regulated by prostaglandin E (PGE), which in turn is regulated by pregnancy specific protein B (PSPB), which is regulated by estradiol-17β and further hypothesized FSH may be the regulatory hormone to placental secretion of estradiol-17β. However, minimal research has been done analyzing FSH and its role, if any, within the theorized model. We hypothesized FSHβ is the hormone responsible for regulating ovine placental estradiol-17β secretion with its cognate receptor (FSHR) present within placentomes.

Two methods of investigation were used to evaluate the expression of FSHβ and FSHR within the ovine placenta. Placentomes from gestational days 53 (n=4) and 101 (n=3) were collected under general anesthesia from Polypay sheep (n=7). Each placentome was manually separated into cotelydonary (fetal) and caruncular (maternal) samples. Real-time polymerase chain reaction (RT-PCR) and immunohistochemistry (IHC) were performed on each sample to

evaluate the quantitative levels of FSHβ and FSHR. Results from RT-PCR and IHC were negative for FSHβ and equivocal for FSHR. However, these findings do not rule out FSHβ expression within the intercotyledonary regions of the placenta or endometrium. Evidence for the presence of FSHR within the placentome was inconclusive, but further studies with larger numbers and improved experimental models, are warranted.

Expression of Follicle Stimulating Hormone (FSHβ) and its Receptor (FSHR) within the Ovine Placentome

By

Eleas M. Wu

A THESIS

Submitted to

Oregon State University

in partial fulfillment of
the requirements for the
degree of

Master of Science

Presented June 5, 2019
Commencement June 2019

Master of Science thesis of Eleas M. Wu presented on June 5, 2019.

APPROVED:

Major Professor, representing Comparative Health Sciences

Dean of the College of Veterinary Medicine

Dean of the Graduate School

I understand that my thesis will become part of the permanent collection of Oregon State University libraries. My signature below authorizes release of my thesis to any reader upon request.

Eleas M. Wu, Author

ACKNOWLEDGEMENTS

The author expresses sincere appreciation to Drs. Charles Estill and William Whitler for their outstanding mentorship both clinically and academically. Your wisdom will always be the "little voice" pointing me in the right direction. Also, I would like to thank the other members of my committee, Dr. Michelle Kutzler for all of her mentorship and countless hours reading revisions and Dr. Marit Bovbjerg for serving as my Graduate Council Representative.

To my wonderful husband, Calvin, for believing in me even when I didn't believe in myself. For his patience and understanding when I had long days at the office and taking care of our family when work and research kept me away.

I especially want to thank the most amazing laboratory team; Dr. Charles Roselli, Rebecka Amodei, Maureen Larson and Kay Fischer for generously taking the time to teach me laboratory procedures and protocols. Last, but certainly not least, Dr. Robert Bildfell for his patience with teaching immunohistochemistry and taking over his office numerous times to use the microscope camera and edit slides. I could not have done this project without any of you!

This project was financially supported from internal funding by Oregon State University Carlson College of Veterinary Medicine and the Fred F. and Corinne McKenzie Memorial Scholarship fund.

TABLE OF CONTENTS

TABLE OF CONTENTS (Continued)

Page

LIST OF FIGURES

LIST OF FIGURES (Continued)

LIST OF FIGURES (Continued)

LIST OF TABLES

LIST OF APPENDICES

LIST OF APPENDIX FIGURES

LIST OF APPENDIX FIGURES (Continued)

LIST OF APPENDIX FIGURES (Continued)

LIST OF APPENDIX FIGURES (Continued)

LIST OF APPENDIX FIGURES (Continued)

LIST OF APPENDIX TABLES

Expression of Follicle Stimulating Hormone (FSHβ) and its Receptor (FSHR) within the Ovine Placentome

1. LITERATURE REVIEW

1.1 Overview of the Ovine Estrous Cycle

Sheep are classically defined as seasonal, polyestrous breeders with consistent 16- to 17-day estrous cycle lengths. Both males and females experience two superimposed annual hormonal patterns. In the Northern Hemisphere, ewes experience a season of anestrus, or absence of estrus, in the spring and summer months followed by a season of cyclicity, or presence of recurring estrus, in the fall and winter (Bartlewski et al., 2011). This seasonal variation occurs due to the brain's response to melatonin levels released by lack of retinal stimulation. Increased melatonin levels inhibit RFamide-related peptide-3 (RFRP-3) expression from the hypothalamus. In short day breeders, RFRP-3 neurons have an inhibitory effect on the levels of kisspeptin (Kiss1), also produced by the hypothalamus. Thus, as daylength decreases, there is an increase in melatonin secretion from the pineal gland, reducing RFRP-3 release. With the reduction of RFRP-3 stimulation, an increase in expression of Kiss1 may occur and gonadotropic activity resumes enabling the ewe to experience regular estrous cycles (Simonneaux et al., 2012).

Regardless of the season, sheep continuously experience neuroendocrine releases of Kiss1, gonadotropin releasing hormone (GnRH), luteinizing hormone (LH) and follicle stimulating hormone (FSH). However, during anestrus, these hormone levels remain at baseline, or below the level of detection, due to a reduction in pulse frequency and amplitude (Driancourt et al., 2000). As cyclicity resumes, FSH levels rise causing follicles to undergo recruitment, selection and dominance, resulting in one or more dominant antral follicles for each wave. The dominant follicle itself secretes estrogen and inhibin from the granulosa cells, both of which assist in atresia of subordinate follicles and facilitate a surge of LH from the

anterior pituitary. As the pre-ovulatory follicle nears ovulation, the frequency of FSH pulses begins to decline while the frequency of LH pulses rise. Ovulation occurs approximately 30 hours after the LH surge (Veiga-Lopez et al., 2008). The corpus luteum (CL) is formed as the granulosa and theca cells transition to large and small luteal cells, respectively. The shift in ovarian steroidogenesis, known as the two-cell two-gonadotropin theory, transitions the ewe from a period of estrogen dominance to one of progesterone dominance (Hillier et al., 1994). This marks the beginning of diestrus, a phase of the estrous cycle lasting approximately 12-15 days if fertilization does not occur and maternal recognition of pregnancy is not established. The CL will undergo luteolysis as a consequence of prostaglandin F_2 alpha ($PGF_{2\alpha}$) release from the endometrium. The $PGF_{2\alpha}$ is transferred from the uterine vein, to the ovarian artery by a countercurrent mechanism and binds to receptors in the CL. Progesterone levels then fall below baseline (< 1 ng/mL) and a new reproductive cycle will occur.

1.2 Maternal Recognition of Pregnancy

Following successful mating and fertilization, the early embryo must signal its presence to the maternal system to prevent luteolysis. The CL is the ovarian structure responsible for the early production of progesterone and is vital to the maintenance of pregnancy. To ensure continued progesterone release by the CL, the uterus must be given a signal to suppress luteolytic pulses of $PGF_{2\alpha}$ released by the endometrium. This signaling mechanism differs between species and is known as maternal recognition of pregnancy (MRP).

In sheep, the luminal epithelium (LE) and superficial ductal glandular epithelium (sGE) are essential for the luteolytic cascade and are responsible for the pulsatile release of

$PGF_{2\alpha}$ from the endometrium (Allison Gray et al., 2000). They are regulated by varying progesterone, estrogen and oxytocin levels and their respective receptors. This regulation begins during estrus (Day 0) when estrogen levels rise, stimulating estrogen receptor alpha (ESR1), progesterone receptor (PGR) and oxytocin receptor (OXTR) expression in the uterine endometrium (Spencer and Bazer, 1995). Following ovulation, elevated progesterone levels "block" the expression of ESR1 and oxytocin (OXT). The continued presence of progesterone throughout diestrus creates a PR downregulation on the endometrial LE and sGE, allowing for the upregulation of ESR1 and OXTR genes (Spencer and Bazer, 1995). This downregulation, combined with oxytocin secretion from the posterior pituitary and the CL, results in the pulsatile release of $PGF_{2\alpha}$ from the endometrial LE and sGE on Days 14-16 (Wathes and Lamming, 1995).

The conceptus must elongate from a spherical to filamentous form and secrete a substance known as interferon-tau (oIFN-tau), beginning on Day 10 and continuing through Day 25 with maximal secretion on Days 14-16 (Spencer et al., 2004). Interferon-tau has anti-luteolytic properties enabling the preservation of the CL with continued production of progesterone for uterine quiescence and pregnancy maintenance. This signaling molecule is synthesized and secreted by the developing trophectoderm acting on the endometrial LE and sGE to suppress ESR1 and OXTR through paracrine factors (Spencer and Bazer, 1996; Fleming et al., 2001). By suppressing OXT, the luteolytic pulses of $PGF_{2\alpha}$ a are inhibited. However, basal production of $PGF_{2\alpha}$ and prostaglandin E_2 (PGE_2) persist. This is due to continued expression of prostaglandin synthase 2 (PTGS2) being released by the endometrial LE and sGE. This production does not cause lysis of the luteal cells and is actually found to be

higher in pregnant than non-pregnant ewes due to an increased production of prostaglandins by the developing ovine conceptus. (Spencer et al., 2004).

1.3 Establishment and Maintenance of Pregnancy

Pregnancy is established and maintained through close endocrinological interactions between the ovary, uterus and developing conceptus. The length of gestation in sheep is 142-152 days (average 147 days), with minor breed variations and day one of gestation considered the first day of breeding. Unlike other ruminant species, the ovine corpus luteum is not maintained throughout the entire gestational period. Prior to Day 90 of gestation, the ovarian tissue (CL) has the principal responsibility of pregnancy maintenance. But during the final 60 days of gestation, the placenta secretes the majority of hormones necessary for pregnancy maintenance.

Following MRP, attachment and placental development begins by Day 15 of gestation (Guillomot, 1995). During this initial developmental stage, the ovine conceptus synthesizes and secretes prostaglandins ($PGF_{2\alpha}$ and PGE). Ironically, ruminant conceptuses produce more prostaglandins than the uterine endometrium, generating higher intraluminal levels in pregnant ruminants as compared with cycling female ruminants (Bazer, 2013). These conceptus-derived prostaglandins play a critical role in gene expression and are important for conceptus elongation (Dorniak et al. 2013; Bazer, 2013). They have both autocrine and paracrine effects within the uterus and conceptus, assisting in the growth and development during the early peri-implantation period.

As gestation progresses, the uterine endometrium undergoes rapid growth and remodeling, specifically during the first 70-80 days of gestation (Guillomot, 1995). This is to support the rapid increase in fetal growth during the second half of gestation. As the

developing conceptus matures, the uterus and placenta evolve through maternal caruncular tissue expansion, increased vascularization, and hyperplasia of the endometrial glands (Bazer, 2013). By Day 60 of gestation, histotroph, or uterine milk, is secreted from the endometrial glands to further aid in nourishment during embryonic development (Roberts and Bazer, 1988).

Concurrently, the uterus is exposed to various hormones responsible for uterine quiescence and embryonic health. It has been proposed by Spencer and Bazer that the sequential exposure of the uterus to estrogen, progesterone, oIFN-tau, placental lactogen (PL), and placental growth hormone (GH) establishes a "servomechanism" (Spencer et al., 2004). This mechanism supports uterine health through remodeling, growth and secretory functions throughout gestation.

1.4 Placentation

1.4.1 Classification

The ruminant placenta is uniquely categorized as non-deciduate, synepitheliochorial (formerly syndesmochorial) cotyledonary placentation. The "syn-" is a consequence of the binucleate giant cell-derived syncytium. Binucleate giant cells (BGC) are exclusive to the ruminant and equid species (Hoffman and Wooding, 1993). They arise from the fetal trophectoderm and modify the uterine epithelium forming syncytial plaques between the fetal and maternal tissues (Wooding, 1982a; Wooding, 1982b; Wooding, 1984).

Synepitheliochorial placentation has three distinct features: the BGC located within the trophectoderm; a feto-maternal syncytium formed by the BGC; and placentomal organization (Wooding and Burton, 2008) These features hastened the subcategorization from epitheliochorial, a categorization denoted for non-ruminants including mares and sows.

1.4.2 Gross Structure

Ruminants have a cotyledonary placentation consisting of a maternal caruncle and fetal cotyledon. Unlike the mare and sow, which exhibit a diffuse distribution of contact between fetal and maternal tissues, ruminants have numerous, discrete areas of attachments, known as placentomes (Wooding and Burton, 2008). The numbers of placentomes present within the uterus vary between ruminant species and can be further categorized as oligocotyledonary or polycotyledonary. Oligocotyledonary placentas contain only 3-8 large placentomes, seen commonly in deer. Cattle, sheep and goats have a polycotelydonary placentation consisting of 20-150 smaller placentomes present throughout the gravid and non-gravid horns (Wooding and Burton, 2008). These placentomal numbers are consistent from one pregnancy to the next.

The caruncular tissue consists of mucosal thickenings within the uterine endometrium visible in both the gravid uterus and non-gravid uterus. These specialized areas are the only sites of nutrient and gas exchange between the maternal tissues and the fetal membranes (cotyledons). Although the physiologic properties are the same, the placentomal structure varies among ruminant species. Bovine placentomes form a convex structure, ovine placentomes are concave, and flattened placentomes are visualized within antelope placentas (Amorosa, 1952).

Ruminants have a non-deciduate placental classification, meaning they do not undergo significant loss of maternal tissue following expulsion of the fetal membranes at parturition. The maternal caruncular tissue undergoes routine uterine involution and remodeling to prepare for another pregnancy.

1.4.3 Histologic Structure

A distinct feature of ruminant placentation is the formation of the binucleate giant cells beginning around Day 14 of gestation. As embryonic development progresses, the binucleate cells mature and invade the caruncular tissues to form syncytia (Wooding and Burton, 2008). By Day 20 of gestation, syncytial plaques cover the entirety of the maternal caruncle (Wango et al., 1990). As the fetal chorionic villi develop and progress toward the maternal tissue, the maternal vasculature matures and pushes toward the chorion. This interconnected web of fetal and maternal tissue and vasculature produce growth and angiogenic factors that support placentomal development.

As the placenta develops, layers of attachment are created, separating the maternal and fetal (chorionic) vasculature. Ruminants have the least invasive form of placentation. Six tissue layers exist: maternal and fetal vascular endothelium, maternal and fetal connective tissue and maternal and fetal epithelium. Each layer plays an important role in pregnancy maintenance and fetal growth and development.

1.5 Placental Hormone Production

Maintenance of pregnancy depends on more than production of progesterone by the CL. Numerous hormones produce a seamless cascade supporting myometrial quiescence and embryonic development. In sheep, the placenta provides progestational support for the majority of pregnancy, producing enough progesterone to support pregnancy by Day 55 of gestation (Cassida and Warwick, 1945). This is a feature unique to the ewe, as other ruminants require the luteal source of progesterone for the entire gestation.

Weems et al. (2007) proposed a model for placental progesterone production; theorizing progesterone secretion is intricately regulated by PGE (Weems et al., 2003), which in turn is regulated by pregnancy specific protein B (PSPB) (Weems et al., 2003), which is

regulated by estradiol-17β (Bridges et al., 1999) and further hypothesized that FSHβ is the regulatory hormone to placental secretion of estradiol-17β.

1.5.1 Progesterone

Progesterone is the hormone responsible for the maintenance of pregnancy in all mammalian species. It creates an environment of uterine quiescence to allow for conceptus growth and development. In most species, progesterone suppresses the surge center of the hypothalamus from releasing GnRH and thus suppressing an LH surge from the anterior pituitary. By reducing LH pulse frequency, supplementary ovulations and subsequent CL development are hindered. The mare is an exception to this rule, as mares may regularly experience diestral ovulations (Stabenfeldt, 1972b). Progesterone, however, does not suppress the hypothalamic tonic center. Low levels of LH and FSH are released from the anterior pituitary stimulating the release of estrogen from antral follicles within the ovarian stroma. However, during pregnancy, the growth of ovarian follicles is reduced, as compared with their growth during the estrous cycle, and it is unknown whether hormone secretion or receptor expression are affected by the decline in follicular activity (Weems et al., 1994).

Progesterone production begins following ovulation and is produced from the precursor molecule, cholesterol. The process is stimulated by LH binding to receptors on the small luteal cells causing an increase in adenylate cyclase and thus cAMP production. Cyclic AMP activates protein kinase A (PKA) to initiate cholesterol transport (Wiltbank et al, 1993). Steroidogenesis begins through the process of transporting cholesterol from the outer mitochondrial membrane to the inner membrane. This is regulated by steroidogenic acute regulatory protein, or StAR, the first of two rate limiting steps (Stocco, 2001). Luteinizing hormone stimulates cytochrome P450 side chain cleavage within the theca cells at the inner

mitochondrial membrane. There, cholesterol is converted to pregnenolone, the second rate-limiting step for gonadal steroid biosynthesis. Pregnenolone is then converted to progesterone through the enzyme 3β-hydroxysteroid dehydrogenase (3β-HSD) (Miller and Auchus, 2011).

Serum progesterone levels do not remain static throughout pregnancy; levels peak around Day 10 of gestation and remain relatively constant until Day 50 of gestation followed by a two-fold rise in progesterone from Days 50-130 of gestation when the fetal-placental unit becomes the necessary component for pregnancy maintenance (Quintero et al., 1995). This phenomenon was confirmed by Cassida and Warwick (1945) after they performed ovariectomies on ewes and concluded the placenta was sufficient for maintenance of pregnancy from Day 55 of gestation to lambing. Prior to Day 55 of gestation, ovariectomized ewes aborted due to insufficient progesterone production (Cassida and Warwick, 1945). Following Day 130 of gestation, levels remain constant (or declined) until lambing (Quintero et al., 1995).

As early pregnancy progresses, the syncytial trophoblast cells begin to produce progestogens. These progestogens are stimulated by an increase in prostaglandin E_1/E_2 production (Weems et al., 2010).

1.5.2 Prostaglandins

Prostaglandins aid in the decrease of progesterone secretion by the corpus luteum at the end of the estrous cycle. In ewes, prostaglandin $F_{2\alpha}$ is secreted by the endometrium on Day 13 of the cycle. The $PGF_{2\alpha}$ is transported locally to the uterine vein and then the ovarian artery through a countercurrent mechanism. The ovarian artery transports the $PGF_{2\alpha}$ to the large luteal cells, where they bind to prostaglandin receptors. Progesterone production is acutely reduced due to the $PGF_{2\alpha}$ causing vasoconstriction and ischemia of the corpus luteum. A lack

of blood flow reduces adenylate cyclase and thus PKA activity, decreasing circulating progesterone levels. The large luteal cells secrete PKC at the time of $PGF_{2\alpha}$ binding, mediating luteolysis through increase of free intracellular calcium uptake, mitogen-activated protein kinase pathways and OXT release (Wiltbank et al., 1989). The small luteal cells have OXTRs. When OXT binds, calcium levels increase and progesterone production is downregulated through apoptosis and regression of the CL (Niswender et al., 2007).

To maintain early pregnancy, prevention of luteolysis is obtained through resistance of the CL, rather than inhibition, to $PGF_{2\alpha}$ (Silvia and Niswender, 1984; Silvia and Niswender, 1986) The resistance is due to PGE_2 through an increase in cAMP and allowing luteal progesterone production to survive (Fitz et al., 1984). Higher concentrations of PGE are established in the uterine venous system during early pregnancy and continue to rise as pregnancy progresses (Weems et al., 2010; Inskeep and Murdoch, 1980; Weems et al., 2003). By Day 90 of gestation, PGE_2, not LH, is solely responsible for progesterone production by the CL (Weems et al., 1997). It is regulated by LH until Day 50 of gestation and PSPB thereafter (Weems et al., 2003).

1.5.3 Pregnancy Specific Protein B

Pregnancy-specific protein B (PSPB) is produced by the syncytial trophoblast cells within the developing placenta, specifically the binucleate giant cells. Production begins early in gestation and is detectable in the maternal serum within the first 30 days of gestation. The function of PSPB is not completely understood, but was once thought to be involved in maternal recognition of pregnancy alongside interferon tau. However, in a study conducted by Weems et al. (2003), there is no evidence PSPB is involved in inhibiting luteolysis. However, it has been proposed to be immunosuppressive and inhibit the maternal immune system until

the fetal-placental unit is mature and able to maintain pregnancy without luteal support (Weems et al., 2003). The concentration of PSPB has been shown to vary depending on fetal numbers. Maternal concentrations of PSPB are higher in twin versus singleton pregnancies in sheep (Willard et al., 1995), goats (Humblot et al., 1990) and cattle (Patel et al., 1995).

Clinically, serum PSPB concentrations are routinely used for the diagnosis of pregnancy. Radioimmunoassay (RIA) testing for the presence of PSPB in serum was first developed in cattle but confirmed effective in sheep in 1988 (Ruder et al., 1988). Since then, it has been a valuable, inexpensive test for early and accurate diagnosis of pregnancy.

Pregnancy-specific protein B has been shown to be a valuable pregnancy hormone with key roles during early pregnancy maintenance through possible immunosuppression and long term through the regulation of PGE_2 and thus progestogens. It has been shown to be regulated by an unlikely pregnancy hormone, estradiol-17β (Weems et al., 1999; Weems et al., 2003).

1.5.4 Estradiol 17-β

Estrogen is critical for early placental development and pregnancy maintenance; playing an invaluable role in supplying blood flow through vasodilation (Liao et al., 2005) and in many species, such as the baboon and pig, it is essential for MRP (Henson et al., 1991; Geisert et al., 2006). For sheep, levels of estradiol-17β continually rise during pregnancy (Findlay and Cox, 1970). However, growth of ovarian follicles is less active within ovarian stroma during pregnancy than during the estrous cycle, suggesting an alternative source (Weems, 1994).

In humans, estrogen is produced by placental tissue and aids in embryogenesis, cell growth, organogenesis and timing of parturition. However, a prohormone,

dehydroepiandrosterone (DHEA) is essential for production. Both maternal and fetal sources support this production with 60% of DHEA produced by the fetal adrenal cortex (Kaludjerovic and Ward, 2012). Although research does not support these claims in sheep, estrogen receptors (ESR1/ESR2) are expressed in both endometrial tissue and utero-placental tissue of pregnant and non-pregnant ewes (Bairagi et al., 2018). The developing placenta produces 80% of the circulating estradiol-17β by Day 90 of gestation (Weems et al., 2004). Further investigations of ovariectomized ewes with $PGF_{2\alpha}$ which generated a sequential increase first in estradiol-17β followed by a rise in PSPB, PGE and subsequently progesterone production (Weems et al., 2007).

During the estrous cycle, estradiol is produced by the granulosa cells within the developing antral follicle by the aromatization of androgens produced by theca cells. This production is regulated by FSH, which acts directly on receptors within the granulosa cells of the developing follicle converting androgens to estradiol-17β. Estrogen, a steroid hormone, is produced from the irreversible conversion of testosterone by the aromatase enzyme.

Although the hormone responsible for the regulation of placental estradiol-17β remains unknown, it has been hypothesized to be regulated by FSH (Weems et al., 2007). The Weems et al. laboratory (2007) performed ovariectomies on ewes at Day 83 of gestation. On Day 90 of gestation, placentomes were harvested and incubated *in vitro* with various hormones specific to pregnancy maintenance, including estradiol-17β. Ovine FSH increased estradiol-17β secretion in both the intact and OVX ewes, suggesting a positive correlation between the two hormones.

1.5.5 Follicle Stimulating Hormone

Weems et al. (2007) originally hypothesized FSH as the regulatory hormone of placental secretion of estradiol-17β during ovine gestation. It is currently unclear if the source

of the FSH and FSHR is of maternal hypophyseal or fetal-placental origin. In rats, expression of LH and FSH receptors on the ovaries during pregnancy showed a marked decline in LH receptors but no change in FSH receptors were observed (Richards, 1980). However, in ewes, hypophysectomies performed after Day 50 of gestation did not affect pregnancy maintenance, suggesting pituitary involvement and thus ovarian receptors are non-essential for the final months of pregnancy (Denamur et al., 1973).

Follicle stimulating hormone is a glycoprotein produced by the anterior pituitary. It is composed of multiple isoforms with significant differences depending on age, sex and reproductive state. Follicle stimulating hormone receptors are expressed on the ovarian granulosa cells aiding in antral follicle development. In addition, FSHR have been detected in extragonadal tissues such as embryos, placenta, endometrium, cervix, and ovarian cancer tissues in humans, cows and mice (Mizrachi and Shemesh, 1999; Shemesh, 2001; Shemesh et al., 2001; Leethongdee et al., 2010; Leethongdee et al., 2014; Stilley et al., 2010; Papadimitrious et al., 2016). In humans, FSHR expression within the endometrium or placental tissue is dependent on the stage of the estrous cycle (La Marca et al., 2005; Stilley et al., 2014).

Luteinizing hormone and FSH are known to be released synchronously in response to a GnRH challenge in nonpregnant ewes (Jonas et al., 1973). In pregnant ewes, FSH concentrations can be measured and detected at Days 42 and 91 of gestation but not at Day 126 of gestation or postpartum in consequence to a GnRH challenge (Chamley et al., 1974a). An increase in circulating FSH levels were appreciated at 6 and 18 weeks (Days 42 and 91 of gestation, respectively), with no significant differences at 18 weeks (Day 126 of gestation) and postpartum. Luteinizing hormone concentrations were also detectable during pregnancy and declined by Day 126 of gestation (Chamley et al., 1974b). The decline in both gonadotropins towards the end of gestation may be due to the lack of follicular activity during pregnancy

(Weems et al., 1994), a refractory maternal pituitary to GnRH during pregnancy or placental derived FSH receptors not regulated by GnRH.

The present experiment was conducted to test the hypothesis of FSHβ as the hormone responsible for regulating ovine placental estradiol-17β secretion via its receptor (FSHR) produced within placentomes. Two methods of investigation, real time polymerase chain reaction (RT-PCR) and immunohistochemistry (IHC), were performed to evaluate the quantitative levels of FSHβ and FSHR.

2. MATERIALS & METHODS

2.1 Animals and Tissue Collection

2.1.1 Sheep

Mature Polypay ewes (*Ovis aries*) (n=7) were synchronized with an intravaginal progestogen (Eazi-breed™ CIDR® Sheep Insert; Zoetis, New York, NY) inserted on day one and treated with cloprostenol 125μg (Estrumate®; Merck Animal Health, Madison, NJ) intramuscularly on day six to regress residual luteal tissue. Each CIDR® was removed on day seven and estrus was detected with an intact ram wearing a marking harness 24-48 hours later. The day of mating was recorded as gestation day (GD) one. In addition, two mature ewes and two mature rams were humanely euthanized for control tissue collection. All experimental procedures and protocols were approved by the Institutional Animal Care and Use Committee guidelines at Oregon State University (See Appendix A (ACUP #5098) and Appendix B (ACUP #4331)) and in accordance with Public Health Services Policy on Humane Care and Use of Laboratory Animals.

2.1.2 Cow

A single mature postpartum Holstein cow (*Bos taurus*) weighing approximately 680 kg was presented to the Oregon Veterinary Diagnostic Laboratory for necropsy and tissue collection following humane euthanasia.

2.1.3 Tissue Collection & Preparation

Anesthesia of each pregnant ewe was induced with ketamine HCl (Ketaset®, Zoetis, Florham Park, NJ) and diazepam (Hospira Inc., Lake Forest, IL) intravenously and then maintained with inhaled isoflurane (Fluriso™; Vet One®, Boise, ID) and oxygen. Ewes were subjected to a ventral midline laparotomy to expose the uterus. An incision was made along

the dorsal curvature of each gravid horn to expose the fetal membranes and developing fetus. Placentomes were obtained on gestation day (GD) 53 ± 2 (n = 4) and GD 101 ± 2 (n = 3) (term: 147 days). Two to four placentomes were removed via sharp transection of the caruncular stalk from the uterus of each ewe adjacent to the attachment of the umbilical cord to the chorioallantois. The placentome was immediately separated into cotyledonary (fetal) tissue and caruncular (maternal) tissue. Tissues were either flash frozen on dry ice or stored in RNAlater™ Stabilization Solution (ThermoFisher Scientific, Waltham, MA) and rapidly frozen at -20ºC and stored at -80ºC until used for RNA extraction. Whole placentomes were also fixed in either 10% neutral buffered formalin (GD 53 placentomes) or 4% paraformaldehyde in sucrose (GD 101 placentomes) until used for immunohistochemistry.

A non-synchronized adult ewe (n=2) and mature rams (n=2) were induced with general anesthesia as described previously with the exception that following tissue collection, they were euthanized with an overdose of barbiturate while still under general anesthesia. Liver, anterior pituitary (oMAP) and ovarian and testicular tissue were collected, fixed in 4% paraformaldehyde in sucrose, and stored at 4ºC. Samples were submitted to the Oregon Veterinary Diagnostic Laboratory (OVDL) Histopathology Department and processed on Tissue-Tek VIP5 Tissue Processor (Sakura, USA), and embedded in Paraffin Type 9 (Richard-Allen Scientific, USA).

Bovine tissues (liver, anterior pituitary (bMAP), and ovary) were collected following humane euthanasia. The tissue samples were fixed in 10% neutral buffered formalin and submitted to the OVDL Histopathology Section for paraffin embedding as described previously.

2.2 Real-time Polymerase Chain Reaction (RT-PCR) Analysis

2.2.1 Total RNA Extraction

Total RNA was extracted from each sample using TRIzol™ Reagent (ThermoFisher Scientific, Waltham, MA) according to the manufacturer's instructions. Briefly, the tissue was homogenized in one milliliter TRIzol™, using a Brinkmann Homogenizer (ThermoFisher Scientific) for one minute. The lysed product was then phase separated using chloroform and centrifuged at 12,000Xg for 15 min. The aqueous phase, containing the RNA, was removed, the RNA precipitated in 2-propanol and pelleted by centrifugation at 12,000Xg for 8 min. The RNA pellet was washed with ice cold 75% ethanol to purify it, then air dried. The final RNA pellet was reconstituted in 50 µL DEPC (RNAse/DNAse-free) water. 50U of RNAse Inhibitor was added and RNA was then tested for quality (see below) and stored at -80C.

2.2.2 RNA Quantity and Quality

The RNA concentration per sample was measured using the optical density of a spectrophotometric reading at absorbance maxima, A260/A280 nm wavelength. A NanoDrop™ 1000 3.7 Spectrophotometer (ThermoFisher Scientific, Wilmington, DE) was used to make measurements in each sample. A260 measures nucleic acids, while A280 measures proteins within the sample. Thus, A260/A280 determines RNA purity, with pure RNA have a ratio between 1.9 and 2.1 in DEPC water. All samples used in the following experiments had ratio > 1.8 i.e. minimal protein contamination.

The integrity of sample RNA was verified with electrophoresis. A 1.2% agarose gel was prepared in 1X MOPS buffer and ethidium bromide (1 µL/mL). DNA was added to the appropriate amount of 6X loading buffer (e.g. 5 µL of PCR product and 1 µL of 6X loading buffer) and loaded on either side of the gel. Size markers (100 bp or 1 kb ladders, Invitrogen) were also loaded. Mini-gels (50 mL) were run at 80 Volts for 10-15 min and larger gels (250 mL) were run at 190 Volts for the time required to obtain satisfactory separation, typically 45

minutes. The DNA was visualized under UV light on a transilluminator and photographed with a digital system (UVP).

2.2.3 Reverse transcription (RT)

The RNA in each sample was normalized to a concentration of 62.5 ng/µL. Complementary DNA (cDNA) was synthesized from RNA by reverse transcription using SuperScript ® III First-Strand Synthesis Kit (Invitrogen, ThermoFisher Scientific, Waltman, MA) according to the manufacturer's instructions. For each sample, 1 µL of Oligo $(dT)_{20}$ primer, 1 µL dNTPs, and 8 µL of RNA (500 ng) was combined and preheated to 65ºC for 5 min. A master mix of SuperScript® enzyme, buffer, MgCl, DTT and RNAse OUT were added to each sample and the synthesis was carried out at 50 ºC for 50 min. The reaction was terminated by heating to 85 ºC for 5min. RNAse H was then added to each sample at 37 ºC for 20 min. The resulting cDNA samples were stored at -20ºC until evaluated.

2.2.4 Quantitative real time PCR (qPCR)

To detect expression levels of *FSHβ, FSHR, CAS, ESR1, ESR2, CYP19 and GAPDH* forward and reverse primers sequences were designed to amplify DNA across exon boundaries using the NIH Primer-BLAST program (see Table 1). All samples reactions were run in triplicate using PowerSYBER™ Green Master Mix (Invitrogen, ThermoFisher Scientific). The total amount of master mix required for all samples was prepared in a separate Eppendorf tube (i.e. for each tube there is 10 µL SYBR + 0.6 µL primer (mix of 10uM Forward and 10 µM Reverse primers –making the final concentration 300nM) + 5.4 µL DEPC H2O). An aliquot of the Master Mix (16 µL) + 4 µL of undiluted transcript was then added to appropriate wells in a 96-well PCR plate. The plate was then sealed with parafilm. The qPCR

was conducted with a QuantStudio™ 7 Real-Time PCR System (Applied Biosystems, Life Technologies, Germany). Reactions were amplified using the following conditions: pre-incubation heating period at 95ºC for 10 min, followed by amplification of 45 cycles at 95ºC for 15 s and 60ºC for 1 min. Melt curves were then performed with a single cycle of 95ºC for 15 s and 60ºC for 1 min. Temperature readings were collected as the temperature ramped back up to 95ºC for 15 s. Finally, samples were cooled to 4ºC. Following completion of all cycles, data acquisition was performed by obtaining the crossing-point-PCR cycle (Ct) values, amplification curves and melting curves. The Ct (cycle threshold) is defined as the number of cycles required for the fluorescent signal to cross the threshold (i.e. exceeds background level). The auto threshold is determined by the QuantStudio™ software for each assay. For all genes a uniform indicated a single PCR product was amplified. Negative control reactions, non-template control (NTC) and minus reverse transcriptase (MRT), were run at the same time to verify the primers were specific for amplified product and the RNA was not contaminated with genomic DNA, respectively.

2.2.5 Data Analysis Using the Delta Delta Ct Method for Relative Quantification

2.2.5.1 Relative Quantification of RNA

Relative mRNA expression of each transcript of interest was calculated according to the "delta-delta Ct Method" ($2^{-\Delta\Delta Ct}$) was used to calculate fold gene expression relative to GD53 cotyledons. Calibrator cDNA pools were run in each assay to allow for comparisons among reactions. Pools varied according to the gene measured, adult sheep pituitary for: *FSHβ*. *FSHR* and *CAS*; adult sheep testes: *ESR1*, *ESR2* and *CYP19*.

2.2.5.2 Melting Curve Analysis

Melting curve analysis was utilized to ensure that the expected amplicon was achieved in the qPCR and detect interference of primer-dimer formation or amplification of a nonspecific product. See Appendix C for complete melting curve plots.

2.2.6 Standard Curve Construction and Primer Efficiencies

Standard curves were constructed using a 1:2 dilution of cDNA and doing a 1:4 serial dilution until there are at least 5 points (i.e., 1:2; 1:8; 1:32; 1:128 and 1:512) on the curve. All standard curves for each primer pair were run using the same qPCR protocol as described previously. Ct values were acquired and plotted against increasing dilution to construct a standard curve, Primer efficiencies were then calculated from the slope of the standard curve for each primer set (i.e. efficiency =10^(-1/slope)). Primer efficiencies for all genes were 92% or greater (see Table 2), confirming validity of using the delta delta Ct method.

2.3 Immunohistochemistry (IHC) Analysis

2.3.1 Sample Preparation & Antigen Retrieval

Paraffin blocks were sectioned at 4-5 µm onto charged slides and baked at 60°C for one hour. Slides were deparaffinized through two changes of xylene and then rehydrated through two changes of 100% ethanol and one change of 80% ethanol in water. Citrate antigen retrieval was performed in a microwave pressure cooker (Viking Tender cooker) using Dako Target Retrieval solution (s1699) for 10 min after pressure was reached. The pressure cooker was slowly vented and the container containing the slides was allowed to sit for 20 min at room temperature.

After antigen retrieval, the tissues were manually treated with 3% hydrogen peroxide (Sigma-Aldrich, St. Louis, MO) to block endogenous peroxidase activity, rinsed with tris-

buffered saline with Tween 20 (TBST) (Biocare Medical, TWB945M) for five min at room temperature followed by an ImmunoBioScience serum-free protein block (AR-6581-02) for 10 min at room temperature to reduce non-specific background staining.

2.3.2 Immunoexpression of FSHβ and FSHR

FSHβ immunostaining was performed using mouse anti-FSHβ monoclonal antibody (#MA5-12144, ThermoFisher Scientific, Waltham, MA, USA) at 1:500 dilution. Antibody specificity had not yet been validated for sheep. To ensure efficacy of the antibody on ovine tissue, MAP (positive control for FSHβ) and liver (negative control) from both sheep and cow were tested. FSHR immunostaining was performed using rabbit anti-FSHR polyclonal antibody F3929 (Sigma Aldrich, St. Louis, MO) at 1:200 dilution. Antibody specificity had previously been validated in sheep (Grazul-Bilska AT et.al, 2018). Ovine ovary and liver were used as positive and negative controls for FSHR.

The primary antibody was diluted in ImmunoBioScience antibody diluent (#AR-6562-02, ImmunoBioScience, Mukilteo, WA, USA) and applied for 30 min at room temperature. Incubations were done in humid chambers at room temperature for 30 min. After washing in TBST, One Step HRP polymer anti-Mouse & Rat IgG (#IH-8062-custom-OrSU, ImmunoBioScience, Mukilteo, WA, USA) was applied to the slides treated with FSHβ for 10 min and One Step HRP polymer anti-Rabbit IgG (#IH-8064-custom-OrSU, ImmunoBioScience, Mukilteo, WA, USA) was applied to the slides treated with FSHR for 7 min at room temperature and then washed in TBST. The chromagen Nova Red™ Substrate Kit (Vector® Laboratories, Burlingame, CA, USA, SK-4800) was applied for five min. Slides were then rinsed in distilled water and counterstained with Gill™ Hematoxylin (ThermoFisher Scientific, Waltman, MA, USA) diluted 1:10 in distilled water for five min. Slides were then

rinsed in distilled water and rinsed in TBST. Samples were then dehydrated in a graded ethanol baths followed by xylene processing and cover slipping.

2.4 Statistical Analysis

No statistical analysis was performed due to few data points.

Table 1. Primer sequences for real time PCR			
	Sense (5' to 3')	**Antisense (3' to 5')**	**PCR Product Length**
GAPDH	GAACGGGAAGCTCGTCATC	TGGACTCCACCACGTACTC	107 bp
FSHβ	TGCCCAGGATGAAGTCCGTCCAGT	ACCAAGTCCCGGGTGTAGCAAT	175 bp
FSHR	GGCCAACAACCTGCTATACATC	GCTGGCAAGTGCTTAATACC	99 bp
CAS (LH/FSHα)	CTCCAGCGAGGTCTAAGAAG	CACTGTGGCCTTGGTAAATG	93 bp
ESR1	ACCGAAGAGGAGGGAGAATG	CCGGGCTGTTCTTCTTAGTG	146 bp
ESR2	GCCGCCCCACGTGCTCATGA	TGAGCTCCACGAAGCCCGGGA	140 bp
Cyp19	GTGTCCGAAGTTGTGCCTATTG	AAGTAGCTGGGACCTGGTATTG	110 bp

Table 1. Primer sequences used in real-time polymerase chain reaction (RT-PCR).

Table 2. Primer efficiencies for real time PCR.	
Primer	**Efficiency (%)**
GAPDH	92.7
FSHβ	94.3
FSHR	100.1
CAS (LH/FSHα)	92.4
ESR1	97.7
ESR2	99.5
CYP19	100.8

Table 2. Primer efficiencies used for real-time polymerase chain reaction (RT-PCR).

3. RESULTS

3.1 Experiment One: Gene Expression in Sheep Placenta

Quantitative PCR was performed to detect gene expression of *FSHβ, FSHR, CAS, ESR1, ESR2 and CYP1*9 in caruncular and cotyledonary tissues from ovine placenta. The experiment was originally designed to measure results from four GD 53 and three GD 101 placentas. However, two GD53 samples had unacceptably degraded mRNA when analyzed by electrophoresis and were hence dropped from the study. Of the six genes analyzed only three (*ESR2*, *FSHR* and *CYP19)* had measurable expression of mRNA as detected by qPCR. Expression levels for the other three genes (*FSHβ, CAS and ESR1)* were not quantifiable because the transcribed experimental samples (+RT) Ct values were not sufficiently greater than the Ct values for their controls i.e., mRNA that was not reverse transcribed (-RT). The acceptable difference is a Ct difference of at least seven cycles (Applied Biosystems, 2008). The mean Ct values for the +RT and –RT samples for each gene and tissue are summarized in Table 3. A high –RT value may be due the presence of genomic DNA in the samples. However, the samples were treated with DNAse and the primers were designed to cross exon boundaries, all in order to prevent this. If genomic DNA was present we would expect a larger amplicon product, which was not the case. Thus, we have no conclusive explanation for why these genes were not quantifiable.

3.1.1 Measurable Gene Expression in the Ovine Placenta

The three genes that were detectable were *ESR2* (Fig. 1A&B), *FSHR* (Fig. 2A&B) and *CYP19 (*Fig. 3A&B). In each case a single product of appropriate size was detected in experimental samples. Product in the –RT controls were either not detectable or emerged after > 7 cycles after that in experimental samples. The fold expression of each gene was expressed

relative to the average of GD53 samples (Fig. 4). For the most part, there were no apparent of differences between caruncular and cotelydonary tissues or across gestational ages. One exception may be for CYP19, which was consistently lower in GD101 caruncle than in any other sample.

3.1.2 Undetectable Genes

The three genes that were not detectable in ovine placental tissue were *FSHβ* (Fig. 5A&B); CAS (Fig. 6A&B) and ESR1 (Fig. 7 A&B). In each case a product of appropriate size was detected in both experimental samples and –RT controls. As explained above, these three genes could not be quantified.

3.2 Experiment 2: Immunohistochemistry (IHC)

3.2.1 FSHβ

No immunoexpression of FSHβ was observed with GD 53 (Fig. 8) or GD 101 (Fig. 9) placentomes. FSHβ was strongly expressed throughout the anterior pituitary. The negative control was devoid of staining.

3.2.2 FSHR

Minimal immunoexpression of FSHR was observed with GD 53 (Fig. 10) and GD 101 (Fig. 11) placentomes. However, there was no immunoexpression in the ovary (positive control) so it is difficult to interpret these findings. The negative control was devoid of staining.

Table 3. RT-PCR Primers												
	FSHβ		FSHR		CAS		Cyp19		ESR-1		ESR-2	
	Mean ΔΔCT	Mean -RT	Mean ΔΔCT	Mean -RT	Mean ΔΔCT	Mean -RT	Mean ΔΔCT	Mean -RT	Mean ΔΔCT	Mean -RT	Mean ΔΔCT	Mean -RT
GD53 Cotyledon	27.64	26.96	32.36	Undetectable	36.61	40.92	22.47	35.76	24.23	25.32	34.25	39.87
GD53 Caruncle	27.43	28.26	32.62	Undetectable	37.10	40.42	23.03	38.14	23.00	25.28	32.91	42.12
GD101 Cotyledon	33.32	28.51	35.87	Undetectable	38.21	38.41	22.58	Undetectable	22.81	25.16	35.87	Undetectable
GD101 Caruncle	30.88	28.18	33.96	Undetectable	39.17	40.17	25.08	Undetectable	19.82	25.42	32.16	Undetectable

Table 3. Real-time polymerase chain reaction (RT-PCR) results for six primer sets. All tests were run in triplicates and the mean values of ΔΔCT and negative reverse transcriptase (-RT) are recorded above.

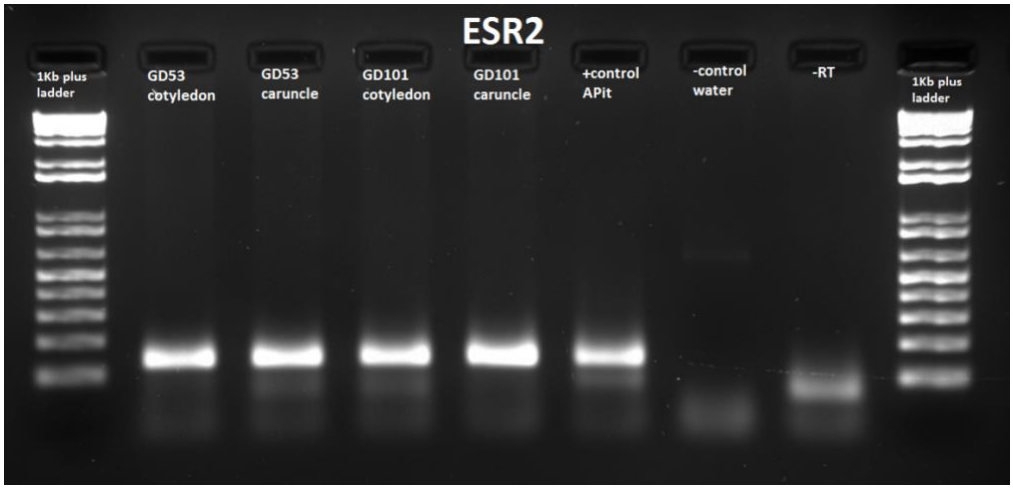

Figure 1A. An ethidium bromide agarose gel electrophoresis (1.2% agarose) of RT-PCR amplified products using species-specific PCR primer sets. The lane on the far left and right are the 1kb DNA ladders. Caruncular and cotyledonary tissues from both gestation day (GD) 53 and 101 evaluated with the ESR2 (estrogen receptor 2) primer. For the positive control anterior pituitary was used and the negative control was sterile distilled water in place of template DNA. The negative RT (-RT) monitors genomic DNA contamination and acts as a second negative control. ESR2 product size is 140 base pairs.

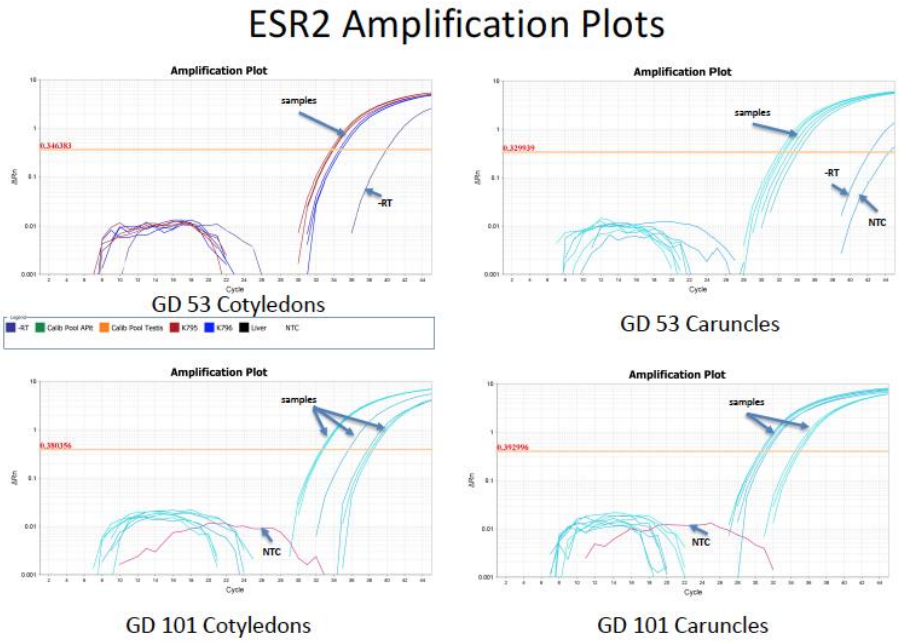

Figure 1B. Estrogen receptor 2 (ESR2) amplification plots for gestational day (GD) 53 and GD 101 experimental samples.

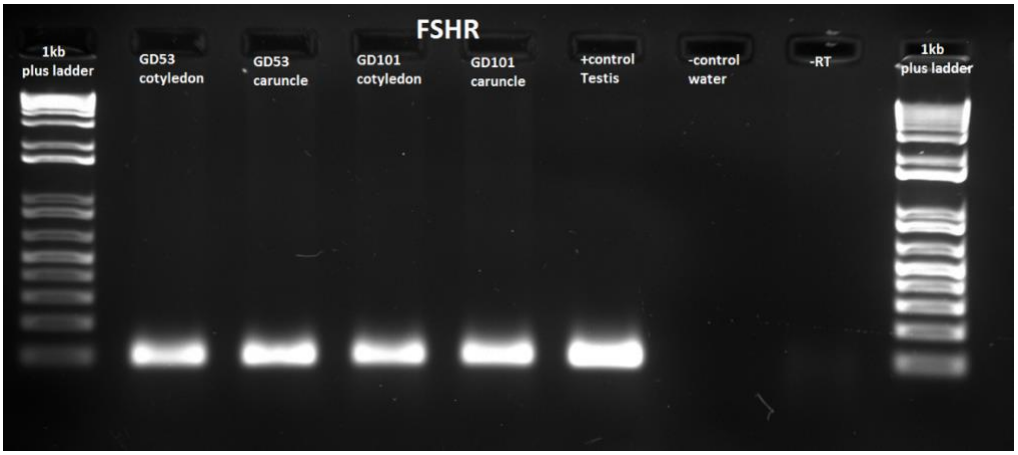

Figure 2A. An ethidium bromide agarose gel electrophoresis (1.2% agarose) of RT-PCR amplified products using species-specific PCR primer sets. The lane on the far left and right are the 1kb DNA ladder. Caruncular and cotyledonary tissues from both gestation day (GD) 53 and 101 evaluated with the follicle stimulating hormone receptor (FSHR) primer. For the positive control, ovine testis was used and the negative control was sterile distilled water in place of template DNA. The negative RT (-RT) monitors genomic DNA contamination and acts as a second negative control. FSHR product size is 99 base pairs.

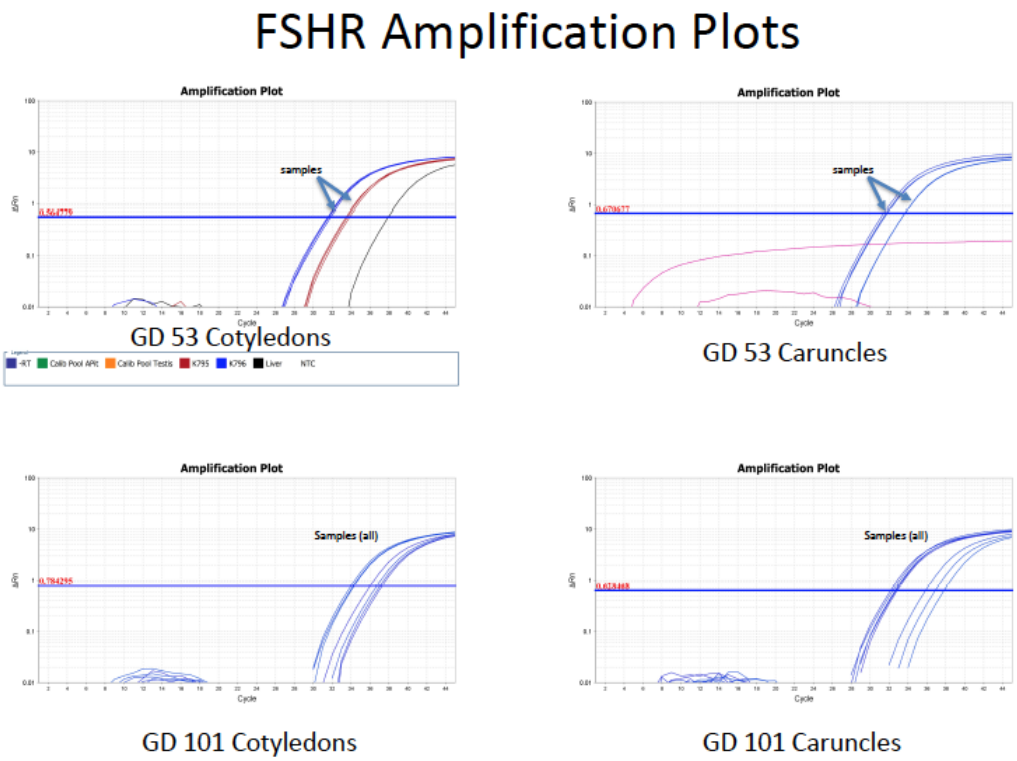

Figure 2B. Follicle stimulating hormone receptor (FSHR) amplification plots for gestational day (GD) 53 and GD 101 experimental samples.

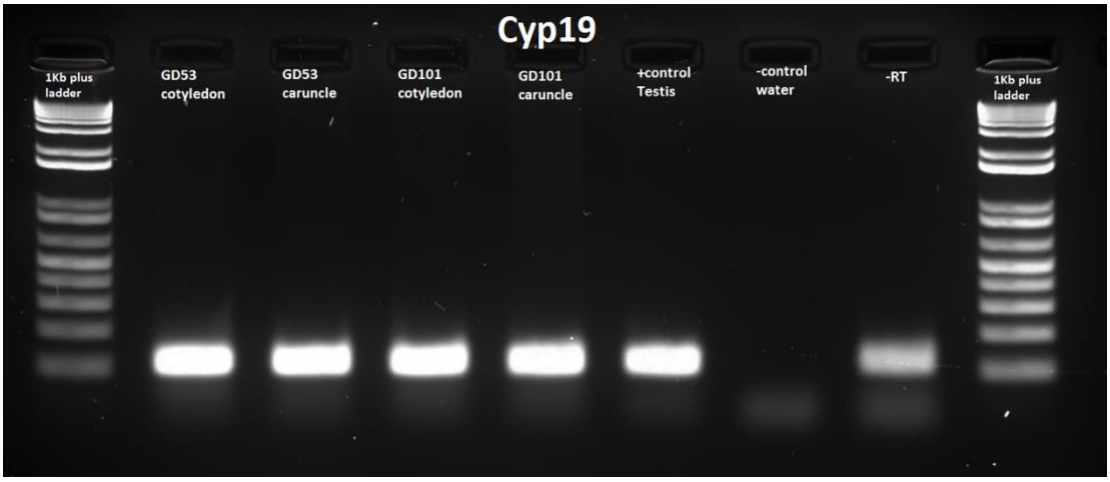

Figure 3A. An ethidium bromide agarose gel electrophoresis (1.2% agarose) of RT-PCR amplified products using species-specific PCR primer sets. The lane on the far left and right are the 1kb DNA ladder. Caruncular and cotyledonary tissues from both gestation day (GD) 53 and 101 evaluated with the CYP19 (aromatase) primer. For the positive control, ovine testis was used and the negative control was sterile distilled water in place of template DNA. The negative RT (-RT) monitors genomic DNA contamination and acts as a second negative control. Cyp19 product size is 110 base pairs.

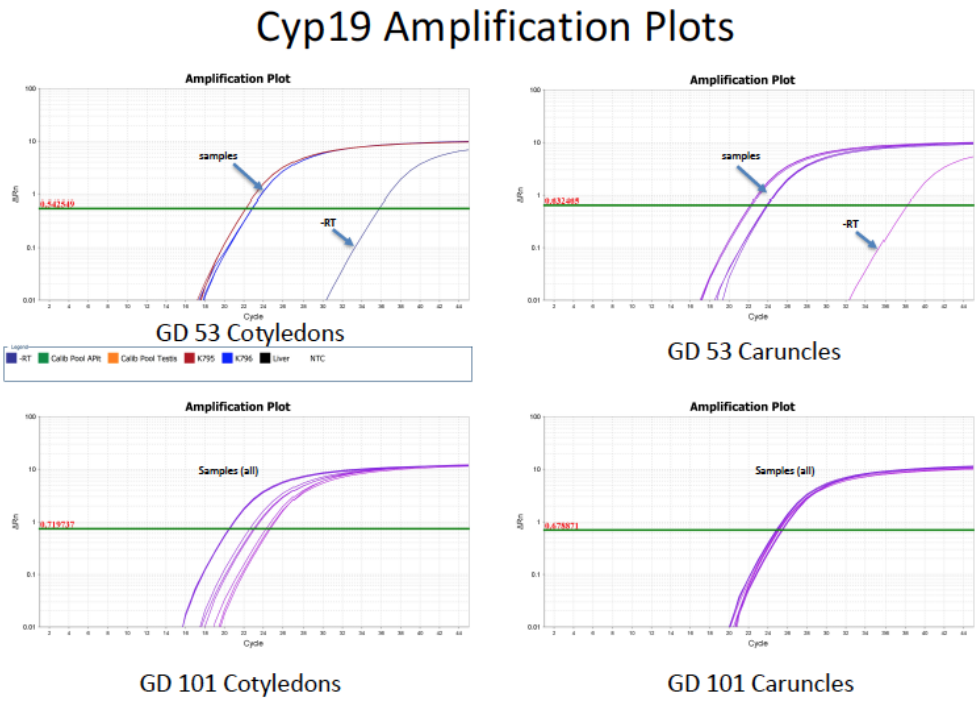

Figure 3B. Aromatase (Cyp19) amplification plots for gestational day (GD) 53 and GD 101 experimental samples.

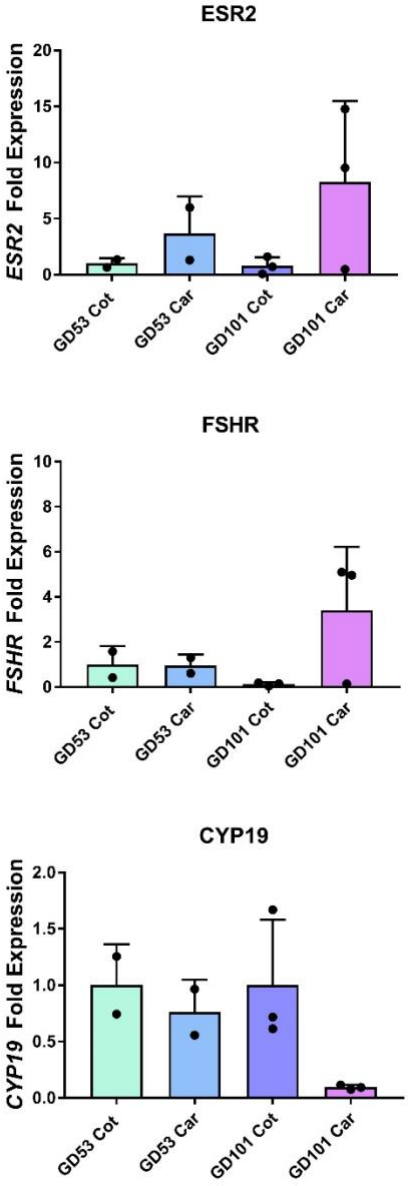

Figure 4. Relative fold expression of estrogen receptor 2 (ESR2), follicle stimulating hormone receptor (FSHR), and aromatase (CYP19) genes in the ovine placenta.

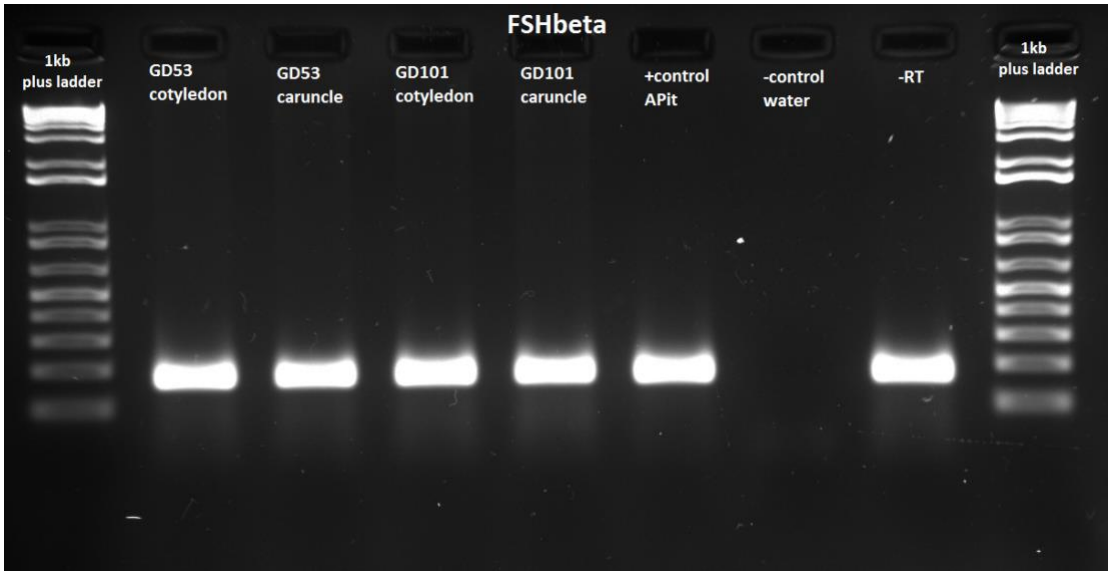

Figure 5A. An ethidium bromide agarose gel electrophoresis (1.2% agarose) of RT-PCR amplified products using species-specific PCR primer sets. The lane on the far left and right are the 1kb DNA ladder. Caruncular and cotyledonary tissues from both gestation day (GD) 53 and 101 evaluated with the follicle stimulating hormone-beta (FSHβ) primers. For the positive control, anterior pituitary was used and the negative control was sterile distilled water in place of template DNA. The negative RT (-RT) monitors genomic DNA contamination and acts as a second negative control. FSHβ product size is 175 base pairs.

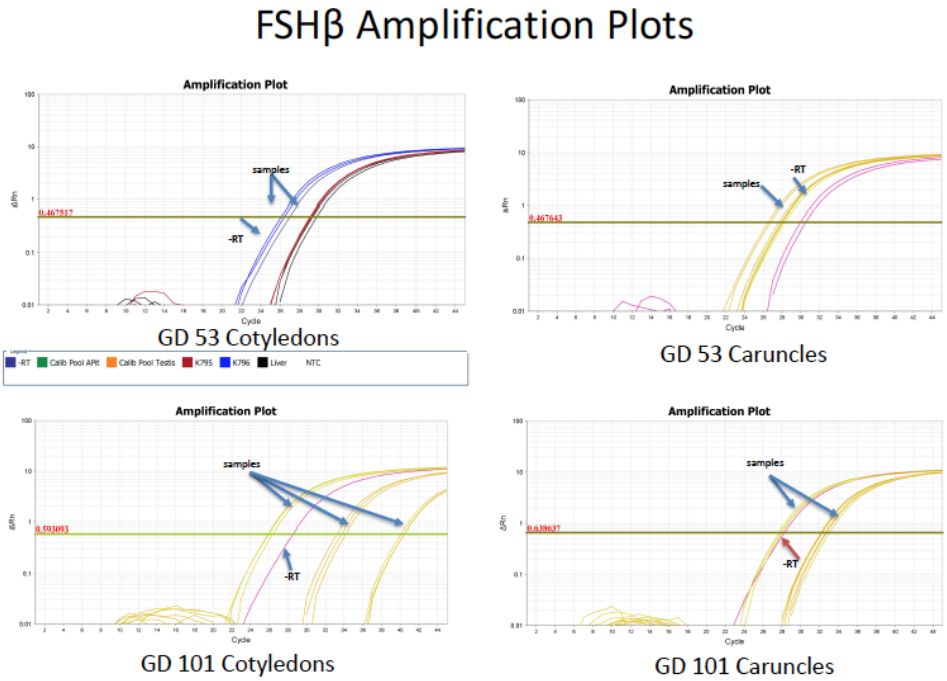

Figure 5B. Follicle stimulating hormone-beta (FSHβ) amplification plots for gestation day (GD) 53 and GD 101 experimental samples.

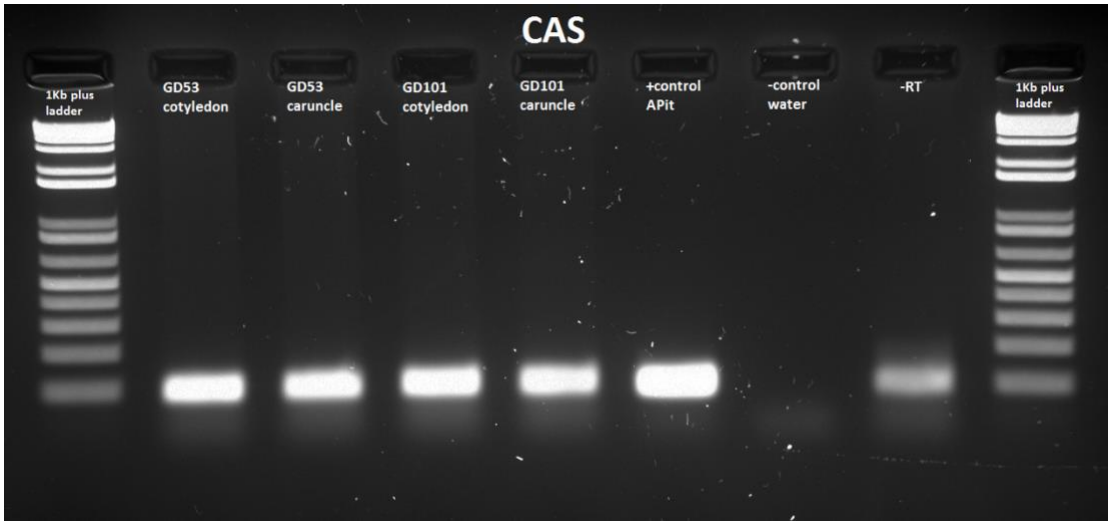

Figure 6A. An ethidium bromide agarose gel electrophoresis (1.2% agarose) of RT-PCR amplified products using species-specific PCR primer sets. The lane on the far left and right are the 1kb DNA ladder. Caruncular and cotyledonary tissues from both gestation day (GD) 53 and 101 evaluated with the CAS (common alpha subunit) primer. For the positive control, anterior pituitary was used and the negative control was sterile distilled water in place of template DNA. The negative RT (-RT) monitors genomic DNA contamination and acts as a second negative control. CAS product size is 93 base pairs.

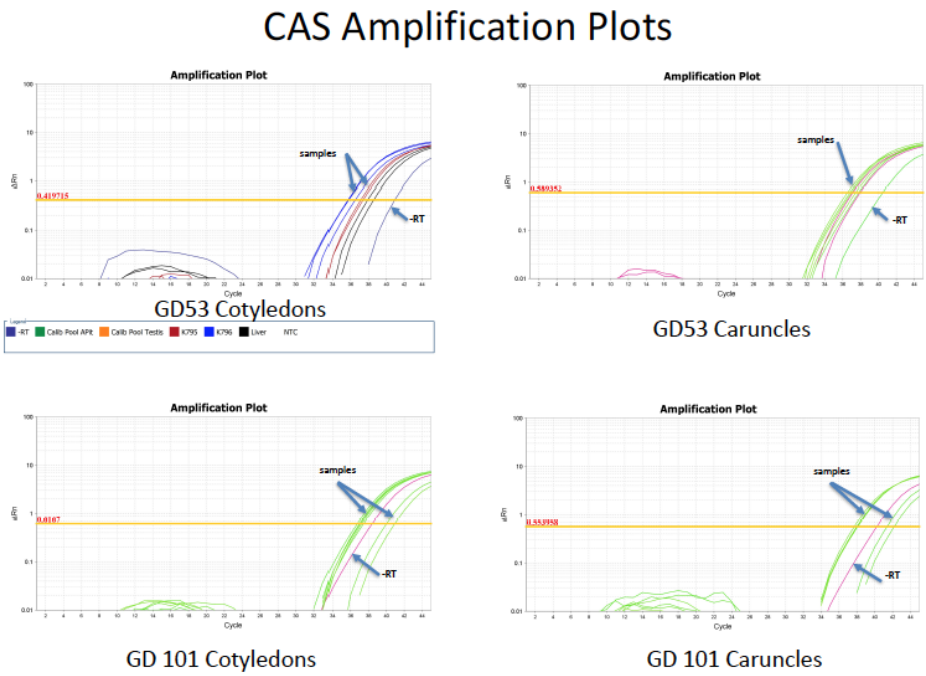

Figure 6B. Common alpha submit (CAS) amplification plots for gestational day (GD) 53 and GD 101 experimental samples.

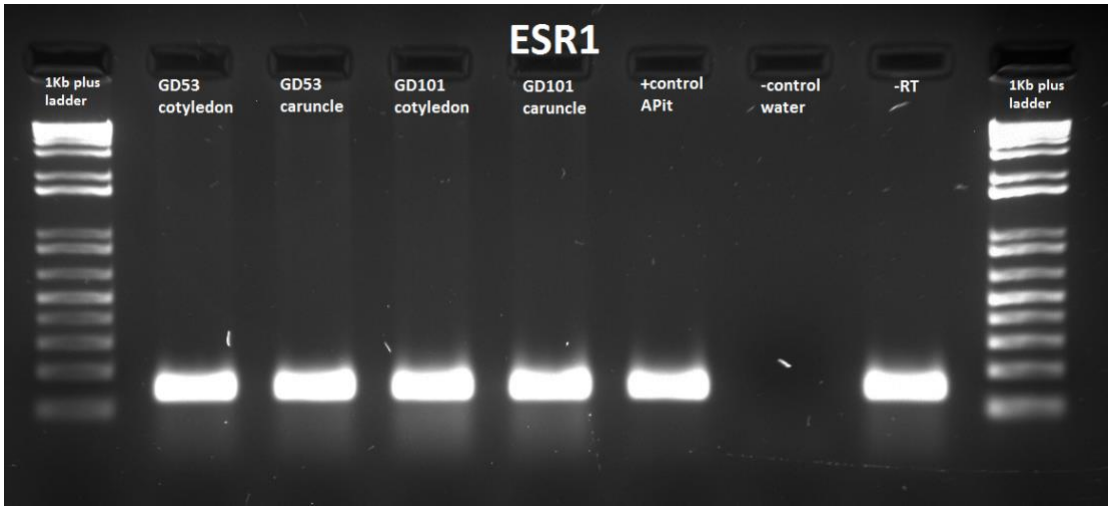

Figure 7A. An ethidium bromide agarose gel electrophoresis (1.2% agarose) of RT-PCR amplified products using species-specific PCR primer sets. The lane on the far left and right are the 1kb DNA ladder. Caruncular and cotyledonary tissues from both gestation day (GD) 53 and 101 evaluated with the ESR1 (estrogen receptor 1) primer. For the positive control, anterior pituitary was used and the negative control was sterile distilled water in place of template DNA. The negative RT (-RT) monitors genomic DNA contamination and acts as a second negative control. ESR1 product size is 146 base pairs.

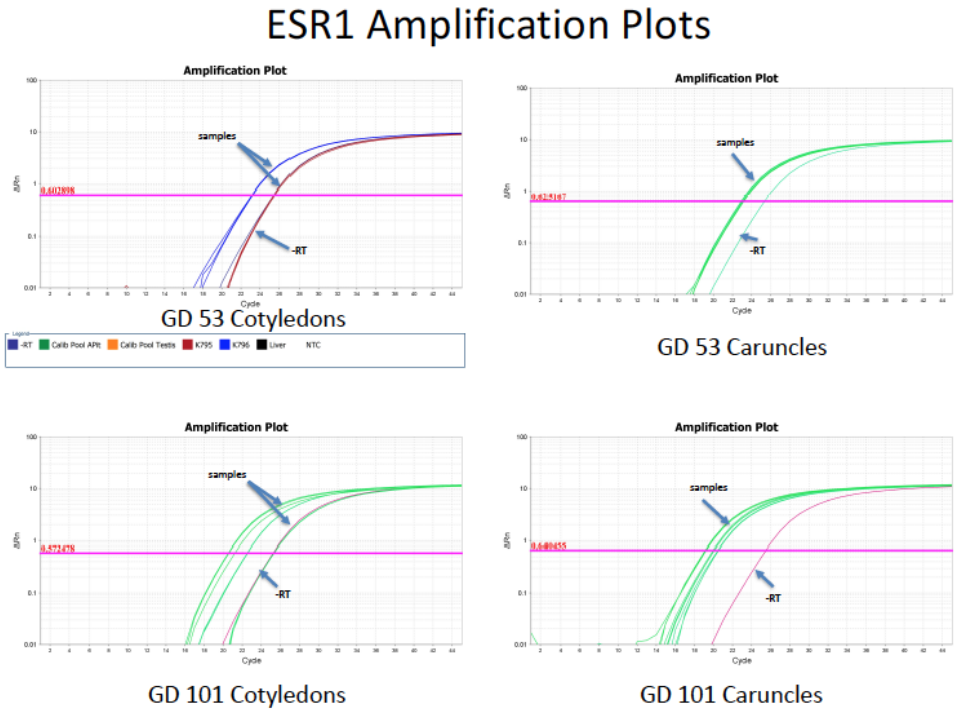

Figure 7B. Estrogen receptor 1 (ESR1) amplification plots for gestation day (GD) 53 and GD 101 experimental samples.

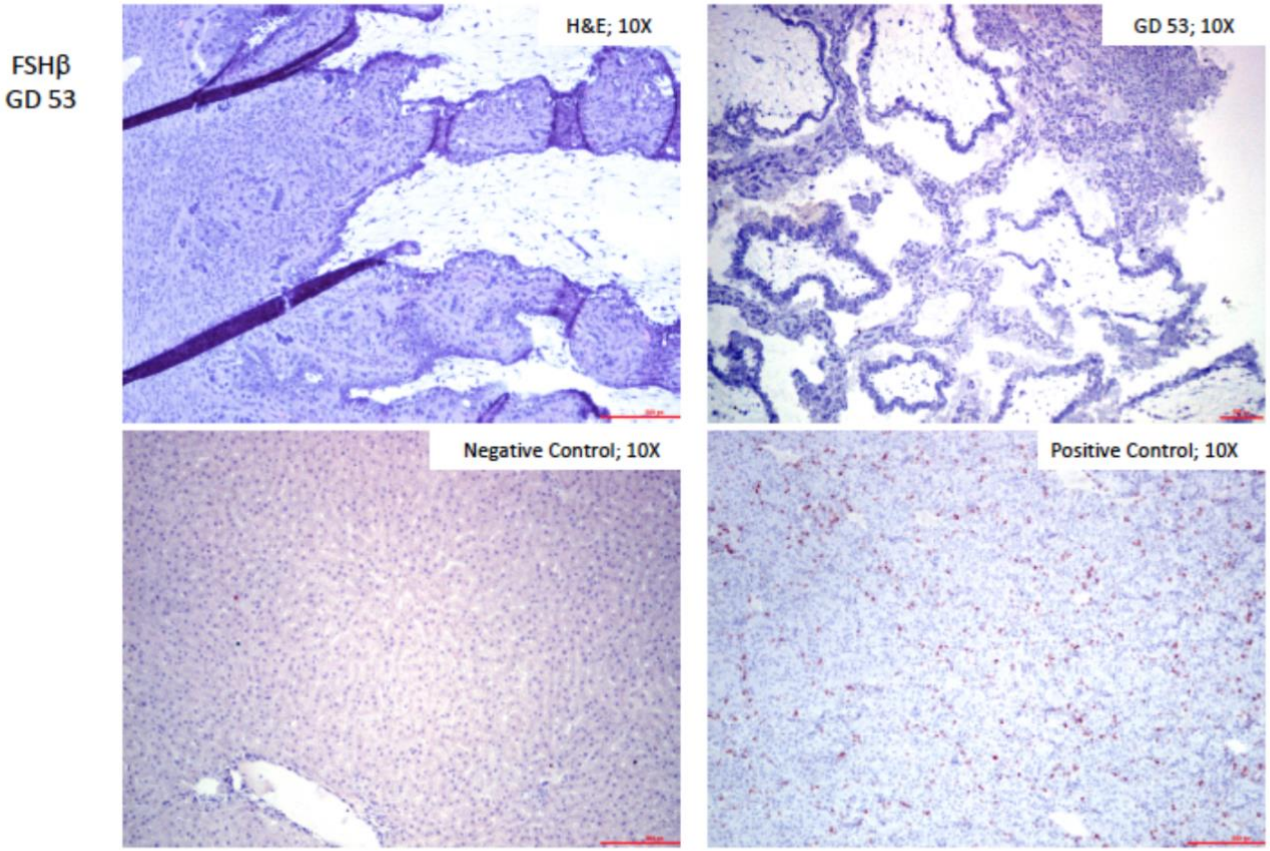

Figure 8. Immunohistochemical analysis showing no immunoexpression for follicle stimulating hormone-beta (FSHβ) on gestational day (GD) 53 (original magnification 10X, upper right). The negative control showed no immunoexpression (original magnification 10X, lower left) and the positive control showed marked immunoexpression (original magnification 10X, lower right). A reference hematoxylin and eosin (H&E) stain of a placentome is in the upper left corner.

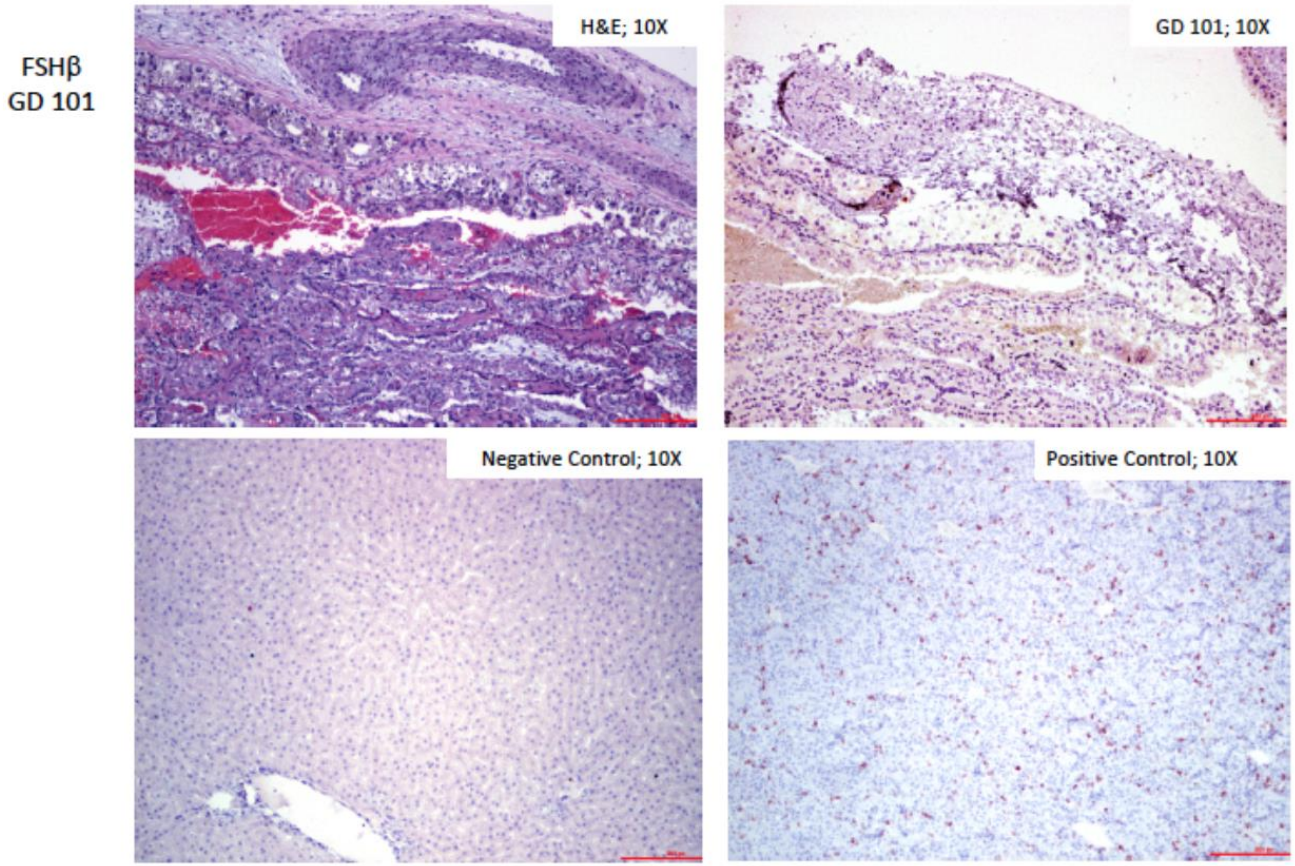

Figure 9. Immunohistochemistry analysis showing no immunoexpression follicle stimulating hormone-beta (FSHβ) on gestational day (GD) 101 (original magnification 10X, upper right). The negative control showed no immunoexpression (original magnification 10X, lower left) and the positive control showed marked immunoexpression (original magnification 10X, lower right). A reference hematoxylin and eosin (H&E) stain of a placentome is in the upper left corner.

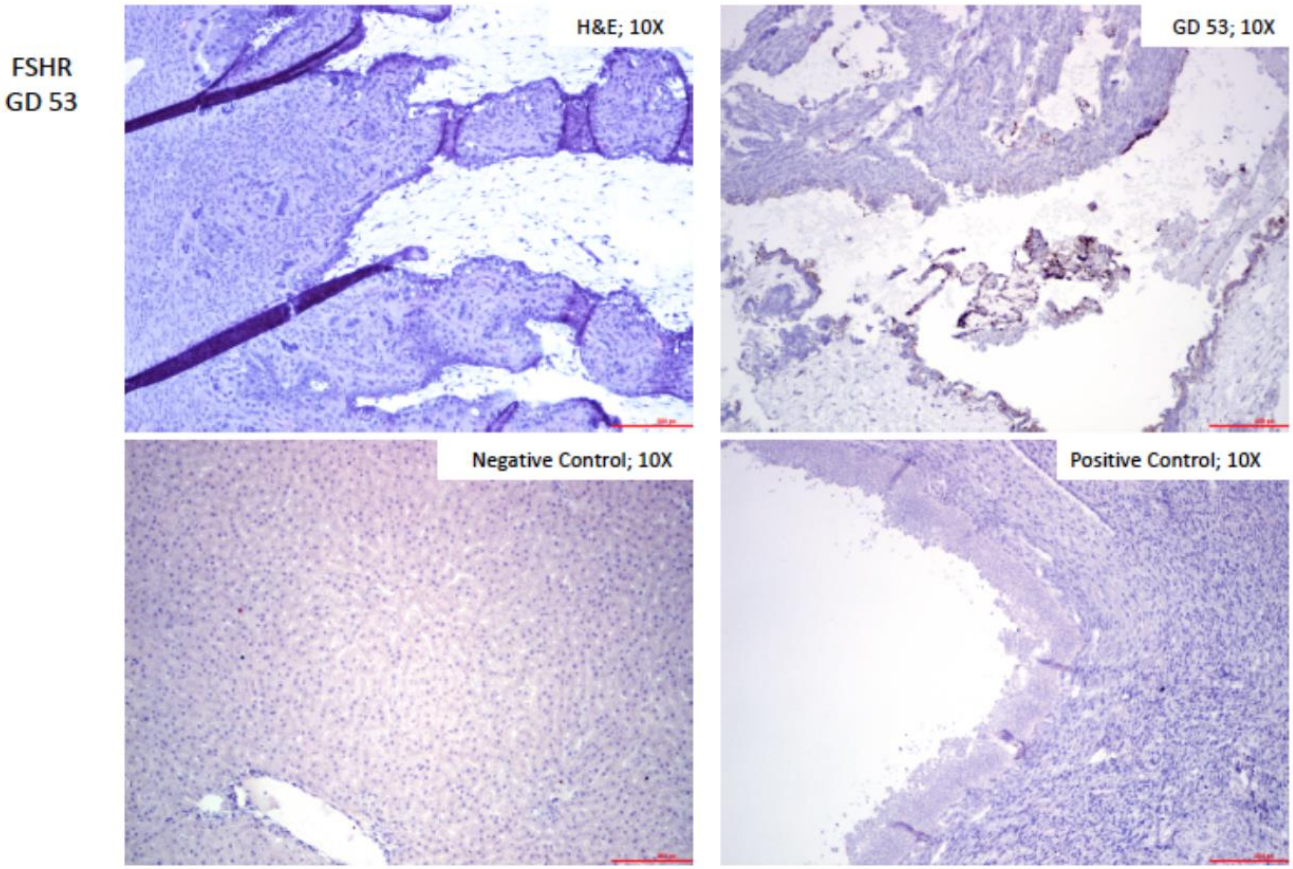

Figure 10. Immunohistochemistry analysis showed inconclusive immunoexpression for follicle stimulating hormone receptor (FSHR) on gestational day (GD) 53 (original magnification 10X, upper right). The negative control showed no immunoexpression (original magnification 10X, lower left) and the positive control showed no immunoexpression (original magnification 10X, lower right). A reference hematoxylin and eosin (H&E) stain of a placentome is in the upper left corner.

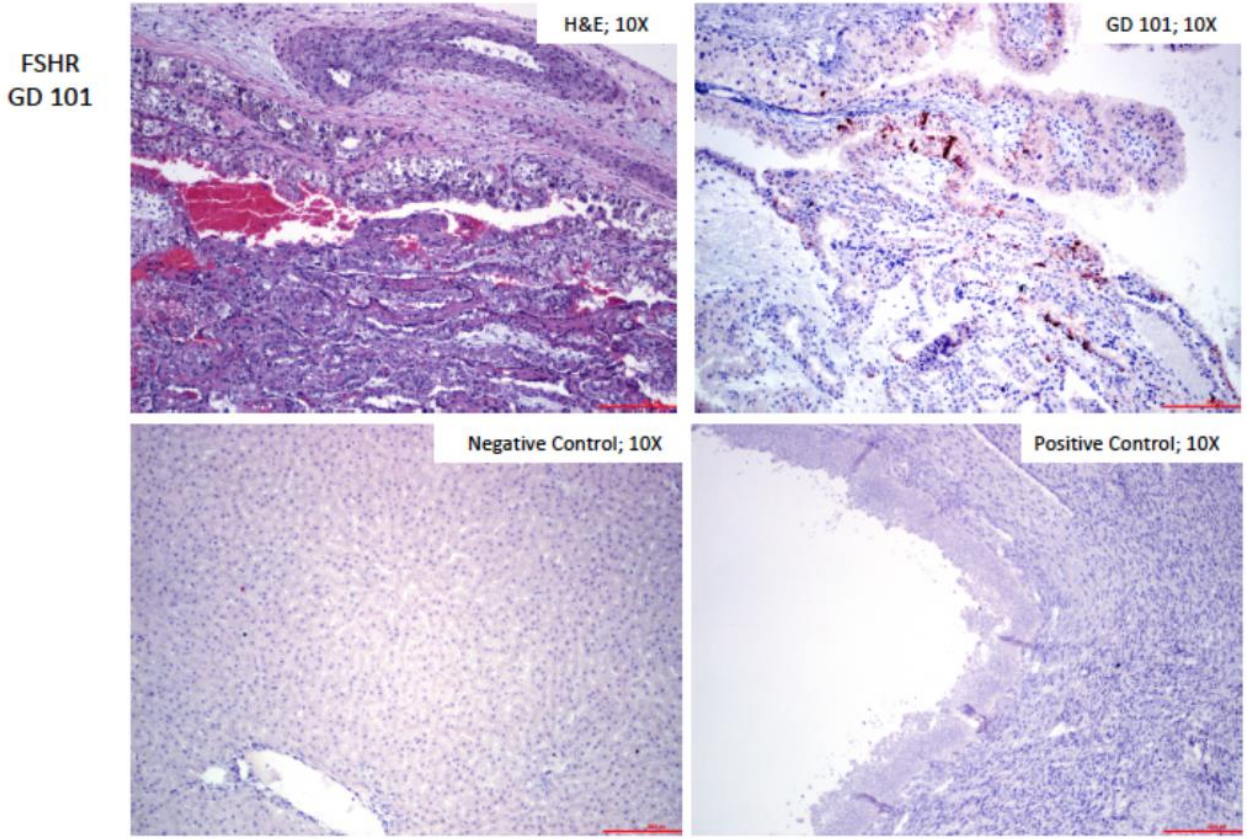

Figure 11. Immunohistochemistry analysis showed inconclusive immunoexpression for follicle stimulating hormone receptor (FSHR) on gestational day (GD) 101 (original magnification 10X, upper right). The negative control showed no immunoexpression (original magnification 10X, lower left) and the positive control showed no immunoexpression (original magnification 10X, lower right). A reference hematoxylin and eosin (H&E) stain of a placentome is in the upper left corner.

4. DISCUSSION

It is well known that progesterone is the hormone responsible for the maintenance of pregnancy in sheep. Prior to Day 90 of gestation, luteal tissue is the principle source of progesterone. As early as GD 55, the placenta secretes the majority of hormones necessary for pregnancy maintenance. By GD 90, the placenta secretes 50% of the circulating progesterone making the ovaries no longer necessary to maintain pregnancy. The current model for placental progesterone production in ewes is an intricately orchestrated cascade of sequential events. The cascade begins with the production of PGE_1 and PGE_2 (Weems et al., 2003), which is regulated by LH prior to GD 50 and PSPB, thereafter (Weems et al., 2003). Pregnancy specific protein B is in turn controlled by placental estradiol-17β (Bridges et al., 1999). In 2007, Weems concluded FSHβ most likely regulates ovine placental estradiol-17β secretion. No further research had been performed on the regulation of placental estradiol-17β during ovine pregnancy. In humans, FSHβ and its receptors (FSHR) have been found in placental tissues as early as 8-10 weeks into pregnancy (Stilley et al., 2014). Our hypothesis was that FSHβ is the agonist of placental secretion of estradiol-17β with FSHR located within the cotyledon-caruncle complex. It was also hypothesized FSHβ may be of placental, rather than pituitary origin.

The results from the experiments in the current study found that FSHβ gene expression and FSHR gene expression were not detectable within the ovine placentomes on GD 53 and GD 101 using immunohistochemistry or RT-PCR. The lack of immunoexpression of FSHR was due to a problem with the antibody, or the experimental design, as the positive control (ovarian follicle) did not demonstrate any FSHR immunoexpression. The lack of immunoexpression of FSHβ could have resulted from the location where samples were obtained (placentomes vs. inter-cotyledonary and caruncular regions vs. endometrium) and/or the gestational age (GD 53 and GD 101). These findings are in contrast with research performed by Stilley et al. (2014) in both mice

and humans. The Stilley et al. (2014) experiments observed FSHR within the placenta (amnion), umbilical cord and maternal decidua (decidual cells and endothelial cells of blood vessels). However, unlike the current study which evaluated an ovine placentome, Stilley et al. (2014) was also able to detect small amounts of FSH mRNA within the placental chorionic plate and myometrium.

In humans, maternal pituitary (MAP) FSHβ synthesis is inhibited during pregnancy (Jaffe et al., 1969). Without the release of FSHβ from the MAP, it is likely FSHβ is produced elsewhere within the body. Although gene expression and immunoexpression were negative for FSHβ within the ovine placentome of the current experiments, the presence of FSHβ within the intercotyledonary-caruncular spaces as well as the maternal endometrium cannot be ruled out. Further, it is unknown on how FSHβ acts to stimulate placental estradiol-17β during pregnancy.

In summary, the results of the present experiment demonstrate the lack of detectable FSHβ and FSHR gene expression within the ovine placentome. Further areas of investigation include the intercotyledonary regions between placentomes and/or uterine endometrium.

5. REFERENCES

Allison Gray C, Bartol FF, Taylor KM, Wiley AA, Ramsey WS, Ott TL, et al. Ovine Uterine Gland Knock-Out Model: Effects of Gland Ablation on the Estrous Cycle. Biology of Reproduction. 2000;62(2):448–456.

Amorosa EC. Placentation. Marshall's Physiology of Reproduction. 1952;2(15):127–311.

Applied Biosystems. Guide to Performing Relative Quantitation of Gene Expression Using Real-Time Quantitative PCR [pamphlet]. 2008.

Bairagi S, Grazul-Bilska AT, Borowicz PP, Reyaz A, Valkov V, Reynolds LP. Placental development during early pregnancy in sheep: Progesterone and estrogen receptor protein expression. Theriogenology. 2018; 114:273–284.

Bartlewski PM, Baby TE, Giffin JL. Reproductive cycles in sheep. Animal Reproduction Science. 2011;124(3–4):259–68.

Bazer FW. Pregnancy recognition signaling mechanisms in ruminants and pigs. Journal of Animal Science and Biotechnology. 2013;4(1):23.

Bridges PJ, Weems YS, Kim LM, LeaMaster BR, Vincent DL, Weems CW. Effect of prostaglandin F2alpha (PGF2alpha), indomethacin, tamoxifen or estradiol-17beta on prostaglandin E (PGE), PGF2alpha and estradiol-17beta secretion in 88 to 90-day pregnant sheep. Prostaglandins & Other Lipid Mediators. 1999;58(2–4):167–178.

Cassida LE, Warwick EJ. The Necessity of the Corpus Luteum for Maintenance of Pregnancy in the Ewe. Journal of Animal Science. 1945;4(1):34–36.

Chamley WA, Findlay JK, Jonas H, Cumming IA, Goding JR. Effect of pregnancy on the FSH response to synthetic gonadotrophin-releasing hormone in ewes. Journal of Reproduction and Fertility. 1974a;37(1):109–112.

Chamley WA, Findlay JK, Cumming IA, Buckmaster JM, Goding JR. Effect of pregnancy on the LH response to synthetic gonadotropin-releasing hormone in the ewe. Endocrinology. 1974b; 94(1):291–293.

Denamur R, Kann G, Short RV. How does the corpus luteum of the sheep know that there is an embryo in the uterus? In: Pierrepont G, editor. Endocrinology of Pregnancy and Parturition, vol. 2. Cardiff, Wales, UK: Alpha Omega Pub Co; 1973. p. 4–38.

Dorniak P, Bazer FW, Spencer TE. Physiology and Endocrinology Symposium: biological role of interferon tau in endometrial function and conceptus elongation. Journal of Animal Science. 2013; 91(4):1627–1638.

Driancourt MA, Fevre J, Martal J, Al-Gubory KH. Control of ovarian follicular growth and maturation by the corpus luteum and the placenta during pregnancy in sheep. Journal of Reproduction and Fertility. 2000; 120(1):151–158.
Findlay JK, Cox RI. Oestrogen in the plasma of the sheep fetus. Journal of Endocrinolology. 1970; 46:281–286.

Fitz TA, Mock EJ, Mayan MH, Niswender GD. Interactions of prostaglandins with subpopulations of ovine luteal cells. II. Inhibitory effects of PGF2 alpha and protection by PGE2. Prostaglandins. 1984;28(1):127–138.

Fleming JA, Choi Y, Johnson GA, Spencer TE, Bazer FW. Cloning of the ovine estrogen receptor-alpha promoter and functional regulation by ovine interferon-tau. Endocrinology. 2001;142(7):2879–2887.

Geisert RD, Ross JW, Ashworth MD, White FJ, Johnson GA, DeSilva U. Maternal recognition of pregnancy signal or endocrine disruptor: The two faces of oestrogen during establishment of pregnancy in the pig. Journal of Reproduction and Fertility. 2006;62(Suppl):131–145.

Guillomot M. Cellular interactions during implantation in domestic ruminants. Journal of Reproduction and Fertility. 1995;49(Supplement):39–51.

Grazul-Bilska AT, Reyaz A, Valkov V, Dorsam ST, Redmer DA. Follicle stimulating hormone receptor protein is expressed in ovine uterus during the estrous cycle and utero-placenta during early pregnancy: An immunohistochemical study. Acta Histochemica. 2018; 120:420–428.

Henson MC, Pepe GJ, Albrecht ED. Regulation of placental low-density lipoprotein uptake in baboons by estrogen: dose-dependent effects of the anti-estrogen ethamoxytriphetol (MER-25)1. Biology of Reproduction. 1991;45(1):43–48.

Hillier SG, Whitelaw PF, Smyth CD. Follicular oestrogen synthesis: the “two-cell, two-gonadotrophin” model revisited. Molecular and Cellular Endocrinology. 1994;100(1–2):51–45.

Hoffman LH, Wooding FB. Giant and binucleate trophoblast cells of mammals. Journal of Experimental Zoology. 1993;559–577.

Humblot P, De Montigny G, Jeanguyot N, Tetedoie F, Payen B, Thibier M, et al. Pregnancy-specific protein B and progesterone concentrations in French Alpine goats throughout gestation. Journal of Reproduction and Fertility. 1990;89(1):205–212.

Inskeep EK, Murdoch WJ. Relation of ovarian functions to uterine and ovarian secretion of prostaglandins during the estrous cycle and early pregnancy in the ewe and cow. International Review of Physiology. 1980; 22:325–356.

Jaffe RB, Lee PA, Midgley AR., Jr. Serum gonadotropins before, at the inception of, and following human pregnancy. Journal of Clinical Endocrinology and Metabolism. 1969; 29:1281–1283.

Jonas HA, Salamonsen LA, Burger HG, Chamley WA, Cumming IA, Findlay JK, et al. Release of FSH after administration of gonadotrophin-releasing hormone or estradiol to the anestrous ewe. Endocrinology. 1973;92(3):862–865.

Kimball FA, Lauderdale JW. Prostaglandin E1 and F2alpha specific binding in bovine corpora Kaludjerovic J, Ward WE. The interplay between estrogen and fetal adrenal cortex. Journal of Nutrition and Metabolism. 2012:837901. doi: 10.1155/2012/837901.

Kimball FA, Lauderdale JW. Prostaglandin E1 and F2alpha specific binding in bovine corpora lutea: comparison with luteolytic effects. Prostaglandins. 1975;10(2):313–331.

La Marca A, Carducci Artenisio A, Stabile G, Rivasi F, Volpe A. Evidence for cycle-dependent expression of follicle-stimulating hormone receptor in human endometrium. Gynecology and Endocrinology. 2005; 21:303–306.

Leethongdee S, Kershaw-Young CM, Scaramuzzi RJ, Khalid M. Intra-cervical application of misoprostol at estrus alters the content of cervical hyaluronan and the mRNA expression of follicle stimulating hormone receptor (FSHR), luteinizing hormone receptor (LHR) and cyclooxygenase-2 in the ewe. Theriogenology. 2010; 73:1257–1266.

Leethongdee S, Khalid M, Scaramuzzi RJ. The effect of the intracervical application of follicle-stimulating hormone or luteinizing hormone on the pattern of expression of gonadotrophin receptors in the cervix of non-pregnant ewes. Reproduction in Domestic Animals. 2014; 49:568–575.

Liao WX, Magness RR, Chen DB. Expression of estrogen receptors-alpha and -beta in the pregnant ovine uterine artery endothelial cells in vivo and in vitro. Biology of Reproduction. 2005; 72:530 – 537.

Miller WL, Auchus RJ. The molecular biology, biochemistry, and physiology of human steroidogenesis and its disorders. Endocrine Reviews. 2011;32(1):81–151.

Mizrachi D, Shemesh M. Follicle-stimulating hormone receptor and its messenger ribonucleic acid are present in the bovine cervix and can regulate cervical prostanoid synthesis. Biology of Reproduction. 1999; 61:776–784.

Moore LG, Ng Chie W, Hudson NL, McNatty KP. Isoforms and half-life of FSH from sheep with different reproductive states. Journal of Endocrinology. 2000;165(2):185–192.

Niswender GD, Davis TL, Griffith RJ, Bogan RL, Monser K, Bott RC, et al. Judge, jury and executioner: the auto-regulation of luteal function. Journal of Reproduction and Fertility. 2007;64 (Suppl):191–206.

Papadimitriou K, Kountourakis P, Kottorou AE, Antonacopoulou AG, Rolfo C, Peeters M, et al. Follicle-Stimulating hormone receptor (FSHR): a promising tool in oncology? Molecular Diagnosis and Therapy 2016; 20:523–530.

Patel OV, Domeki I, Sasaki N, Takahashi T, Hirako M, Sasser RG, et al. Effect of fetal mass, number and stage of gestation on pregnancy-specific protein B concentrations in the bovine. Theriogenology. 1995;44(6):827–833.

Quintero B, Manzo M, Diaz T, Verde 0, Benacchio N, Sifontes L. Seasonal changes in ovarian activity and estrous behavior of Thoroughbred mares in a tropical environment. Biology of Reproduction. 1995;52(monograph_series1):469–474.

Richards JS. Maturation of ovarian follicles: actions and interactions of pituitary and ovarian hormones on follicular cell differentiation. Physiology Reviews 1980; 60:51–89.

Roberts RM, Bazer FW. The functions of uterine secretions. Journal of Reproduction and Fertility. 1988;82(2):875–892.

Ruder CA, Stellflug JN, Dahmen JJ, Sasser RG. Detection of pregnancy in sheep by radioimmunoassay of sera for pregnancy-specific protein B. Theriogenology. 1988;29(4):905–912.

Shemesh M. Actions of gonadotrophins on the uterus. Reproduction. 2001;121,835–842.

Shemesh M, Mizrachi D, Gurevich M, Stram Y, Shore LS, Fields MJ. Functional importance of bovine myometrial and vascular LH receptors and cervical FSH receptors. Seminars in Reproduction Medicine. 2001;19,87–96.

Silvia WJ, Niswender GD. Maintenance of the corpus luteum of early pregnancy in the ewe. III. Differences between pregnant and nonpregnant ewes in luteal responsiveness to prostaglandin F2 alpha. Journal of Animal Science. 1984;59(3):746–753.

Silvia WJ, Niswender GD. Maintenance of the corpus luteum of early pregnancy in the ewe. IV. Changes in luteal sensitivity to prostaglandin F2 alpha throughout early pregnancy. Journal of Animal Science. 1986;63(4):1201–1207.

Simonneaux V, Ancel C. RFRP neurons are critical gatekeepers for the photoperiodic control of reproduction. Frontiers in Endocrinology, 2012.

Spencer TE, Bazer FW. Ovine interferon tau suppresses transcription of the estrogen receptor and oxytocin receptor genes in the ovine endometrium. Endocrinology. 1996;137(3):1144–1147.

Spencer TE, Bazer FW. Temporal and Spatial Alterations in Uterine Estrogen Receptor and Progesterone Receptor Gene Expression During the Estrous Cycle and Early Pregnancy in the Ewe1. Biology of Reproduction. 1995;53(6):1527–1543.

Spencer TE, Burghardt RC, Johnson GA, Bazer FW. Conceptus signals for establishment and maintenance of pregnancy. Animal Reproduction Science. 2004;82–83:537–550.

Stabenfeldt GH, Drost M, Franti CE. Peripheral plasma progesterone levels in the ewe during pregnancy and parturition. Endocrinology. 1972a;90(1):144–150.

Stabenfeldt GH, Hughes JP, Evans JW. Ovarian activity during the estrous cycle of the mare. Endocrinology. 1972b;90(5): 1379-1384.

Stilley JA, Christensen DE, Dahlem KB, Guan R, Santillan DA, England SK, et al. FSH receptor (FSHR) expression in human extragonadal reproductive tissues and the developing placenta, and the impact of its deletion on pregnancy in mice. Biology of Reproduction. 2014;91(74):1–15.

Stocco DM. StAR protein and the regulation of steroid hormone biosynthesis. Annual Review of Physiology. 2001; 63:193–213.
Veiga-Lopez A, Encinas T, McNeilly AS, Gonzalez-Bulnes A. Timing of preovulatory LH surge and ovulation in superovulated sheep are affected by follicular status at start of the FSH treatment. Reproduction in Domestic Animals. 2008; 43:92–98.

Wango EO, Wooding FB, Heap RB. The role of trophoblastic binucleate cells in implantation in the goat: a morphological study. Journal of Anatomy. 1990; 171:241–257.

Wathes DC, Lamming GE. The oxytocin receptor, luteolysis and the maintenance of pregnancy. Journal of Reproduction and Fertility. 1995;49(Suppl):53–67.

Weems, YS. Effects of prostaglandin F2α or trilostane on pregnancy in 90–100 day pregnant sheep. PhD Dissertation, University of Hawaii, 1994.

Weems YS, Vincent DL, Nusser KD, Tanaka Y, Miller-Patrick K, Ledgerwood KS, et al. Effects of prostaglandin F2 alpha (PGF2 alpha) on secretion of estradiol-17 beta and cortisol in 90 to 100 day hysterectomized, intact and ovariectomized pregnant ewes. Prostaglandins. 1994;48(3):139–56.

Weems YS, Bridges PJ, Tanaka Y, Sasser RG, LeaMaster BR, Vincent DL, et al. PGE1 or PGE2, not LH, regulates secretion of progesterone in vitro by the 88–90 day ovine corpus luteum of pregnancy. Prostaglandins. 1997; 53:337–353.

Weems YS, Bridges PJ, LeaMaster BR, Sasser RG, Vincent DL, Weems CW. Secretion of progesterone, estradiol-17beta, PGE, PGF2alpha, and pregnancy-specific protein B by 90-day intact and ovariectomized pregnant ewes. Prostaglandins & Other Lipid Mediators. 1999;58(2–4):139–148.

Weems YS, Kim L, Humphreys V, Tsuda V, Weems CW. Effect of luteinizing hormone (LH), pregnancy specific protein B (PSPB), or arachidonic acid (AA) on ovine endometrium of the estrous cycle or placental secretion of prostaglandins E2 (PGE2) and F2alpha (PGF2alpha) and progesterone in vitro. Prostaglandins & Other Lipid Mediators. 2003;71(1–2):55–73.

Weems YS, Kim L, Tsuda V, Yin C, Weems CW. What regulates placental steroidogenesis in 90-day pregnant ewes? Prostaglandins & Other Lipid Mediators. 2007;84(1–2):54–65.

Weems YS, Nett TM, Rispoli LA, Davis TL, Johnson DL, Uchima T, et al. Prostaglandin E1 (PGE1), but not prostaglandin E2 (PGE2), alters luteal and endometrial luteinizing hormone (LH)

occupied and unoccupied LH receptors and mRNA for LH receptors in ovine luteal tissue to prevent luteolysis. Prostaglandins & Other Lipid Mediators. 2010;91(1–2):42–50.

Willard JM, White DR, Wesson CA, Stellflug J, Sasser RG. Detection of fetal twins in sheep using a radioimmunoassay for pregnancy-specific protein B. Journal of Animal Science. 1995;73(4):960–966.

Wiltbank MC, Belfiore CJ, Niswender GD. Steroidogenic enzyme activity after acute activation of protein kinase (PK) A and PKC in ovine small and large luteal cells. Molecular and Cellular Endocrinology. 1993;97(1–2):1–7.

Wiltbank MC, Guthrie PB, Mattson MP, Kater SB, Niswender GD. Hormonal regulation of free intracellular calcium concentrations in small and large ovine luteal cells. Biology of Reproduction. 1989;41(4):771–778.

Wooding FB. Role of binucleate cells in fetomaternal cell fusion at implantation in the sheep. The American Journal of Anatomy. 1984;170(2):233–250.

Wooding FB. Structure and function of placental binucleate ('giant') cells. Bibliotheca Anatomica. 1982a;(22):134–139.

Wooding FB. The role of the binucleate cell in ruminant placental structure. Journal of Reproduction and Fertility. 1982b;31(Suppl):31–39.

Wooding P, Burton G. Comparative Placentation: Structures, Functions and Evolution. First. Springer-Verlag Berlin Heidelberg; 2008. pp. 133–140.

APPENDICES

APPENDIX A: ACUP #5098

Oregon State University

Institutional Animal Care and Use Committee • Office of Research Integrity
B308 Kerr Administration Building, Corvallis, Oregon 97331-2140 **Phone:** (541) 737-2762
iacuc@oregonstate.edu | http://research.oregonstate.edu/iacuc/

To: Dr. Charles Estill **Home Department:** Clinical Sciences

Protocol ID: 5098 **Protocol Title:** A ram model of neuroendocrine function

Your IACUC Protocol submission has been reviewed and **approved** by the committee.

Protocol Approval Date: **10/16/18**
Annual Expiration Dates: **10/15/19, 10/15/20**
Three-Year (Final) Expiration Date: **10/15/21**
This protocol is not valid if expired. Please submit your renewals in a timely manner.

USDA Research Facility:	PHS Assurance:	AAALAC International:
92-R-0041	D16-00145	Full Accreditation

Maintaining IACUC Protocol approval is contingent upon meeting the policies and standards of our Animal Care and Use Program. Stipulations include but are not limited to the following:

- All participants must be appropriately qualified and experienced to perform work with living animals.
- All proposed changes to an approved IACUC Protocol require review and approval prior to implementation.
- Annual Protocol Reports must be submitted for approval prior to the Expiration Dates above.
- Investigators must avoid or minimize animal discomfort, distress, and/or pain, consistent with sound science and current standards.
- If an animal experiences unexpected pain, distress, morbidity, or mortality, the Attending Veterinarian must be contacted as soon as possible to provide help for the animal.
- Investigators must promptly address Protocol-related incidents, reports, and concerns with the IACUC.

For additional information about the IACUC, please contact our office at (541) 737-2762, send us an email, or visit the IACUC website.

Dr. Chrissa Kioussi
IACUC Chair

Date: 10-16-2018

APPENDIX B: ACUP #4699

Institutional Animal Care and Use Committee • Office of Research Integrity
B308 Kerr Administration Building, Corvallis, Oregon 97331-2140 **Phone:** (541)-737-2762
iacuc@oregonstate.edu | http://oregonstate.edu/research/iacuc/

To: Dr. Fredrick Stormshak
Dept.: Animal and Rangeland Sciences
ACUP Number: **4699**
ACUP Title: A Ram Model of Neuroendocrine Function

Your Animal Care and Use Protocol (ACUP) submission has been reviewed and **approved** by the IACUC.

Approval Date: 05/19/15
Annual Expiration Dates: 05/18/16, 05/18/17
3-Year Expiration Date: 05/18/18

This 3-year **approval is contingent** on maintaining compliance with the policies and standards of OSU's Animal Care and Use Program, which include the following stipulations:

Any **proposed changes** to the approved ACUP require submission of an Amendment Form to the IACUC. Proposed changes must be reviewed and approved prior to implementation.

All **additional participants** must be added to the approved ACUP by submission and approval of a Participant Amendment Form.

An **Annual Review Form** must be reviewed and **approved prior to each Annual Expiration Date**. Any animal activity completed without an approved ACUP in place constitutes significant protocol noncompliance.

Investigators must **contact** the **Attending Veterinarian** as soon as possible to report any unexpected pain, distress, illness, or other animal health concerns.

Investigators are obliged to **report ACUP noncompliance** to the IACUC.

If you would like additional information, please contact the IACUC office at (541) 737-2762, send an email, or visit the IACUC website.

USDA Research Facility #:	PHS (OLAW) Assurance #:	AAALAC Accreditation through
92-R-0005	A3229-01	Fall 2017

Dr. Andrew Buermeyer
IACUC Chair

Date: 05-19-2015

APPENDIX C: MELTING CURVE PLOTS

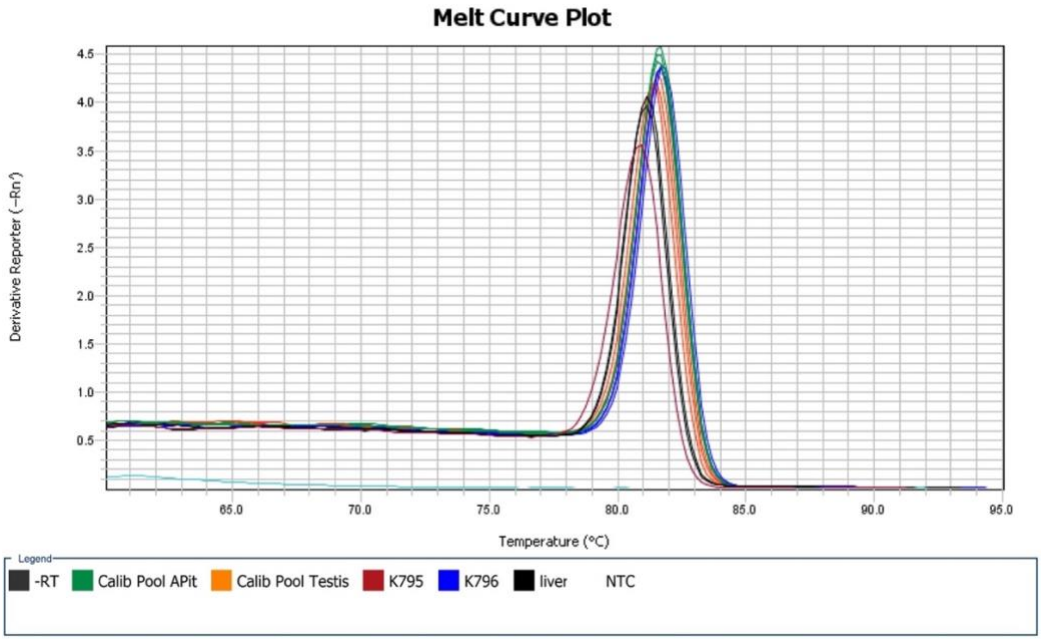

Figure C1a. The melting curve was generated during analysis of the expression of GAPDH within the gestational day (GD) 53 caruncular tissue. The curve is generated at the end of each PCR run showing the specificity of amplification, which is evidenced by a single peak for each mRNA assay. The no template control (NTC) showed no peaks and the signal remained horizontal.

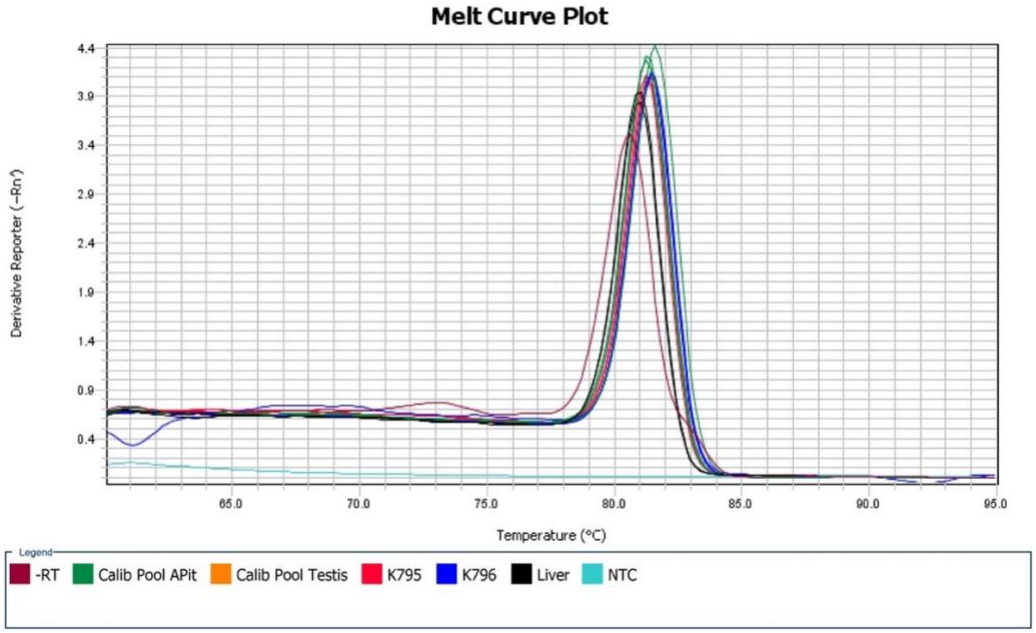

Figure C1b. The melting curve was generated during analysis of the expression of GAPDH within the gestational day (GD) 53 cotyledonary tissue. The curve is generated at the end of each PCR run showing the specificity of amplification, which is evidenced by a single peak for each mRNA assay. The no template control (NTC) showed no peaks and the signal remained horizontal.

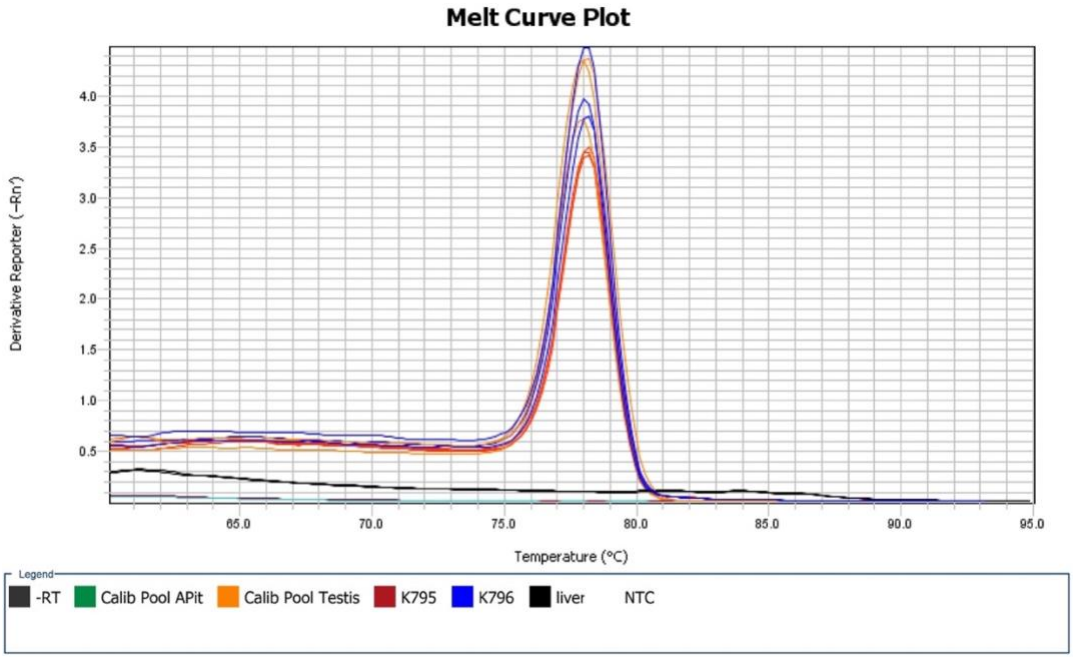

Figure C2a. The melting curve was generated during analysis of the expression of follicle stimulating hormone receptor (FSHR) within the gestational day (GD) 53 caruncular tissue. The curve is generated at the end of each PCR run showing the specificity of amplification, which is evidenced by a single peak for each mRNA assay. The no template control (NTC) showed no peaks and the signal remained horizontal.

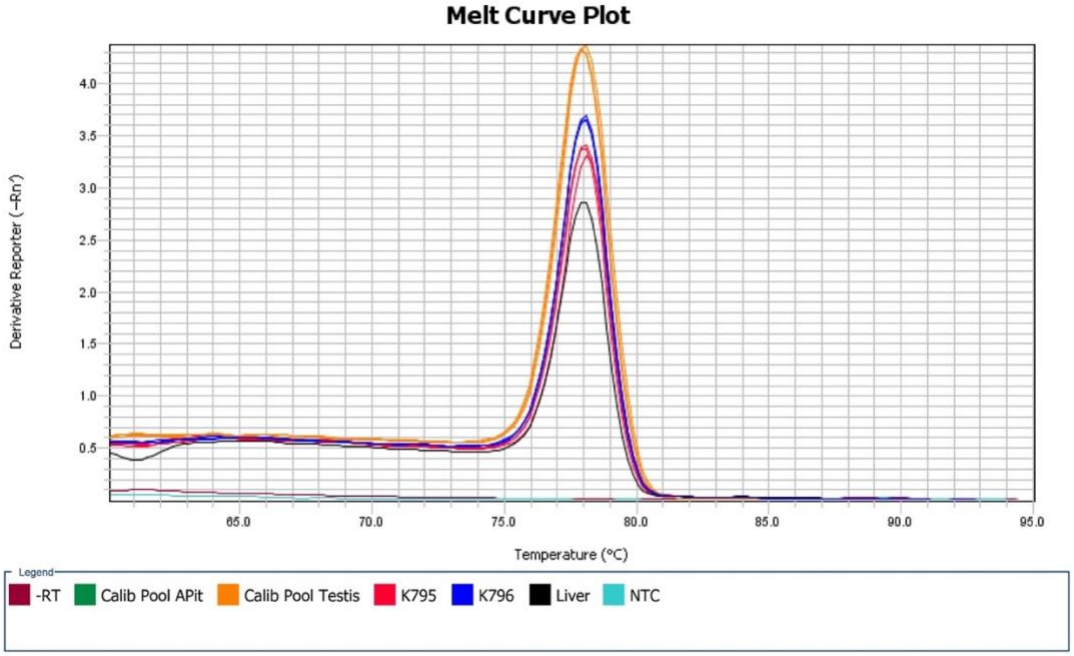

Figure C2b. The melting curve was generated during analysis of the expression of follicle stimulating hormone receptor (FSHR) within the gestational day (GD) 53 cotyledonary tissue. The curve is generated at the end of each PCR run showing the specificity of amplification, which is evidenced by a single peak for each mRNA assay. The no template control (NTC) showed no peaks and the signal remained horizontal.

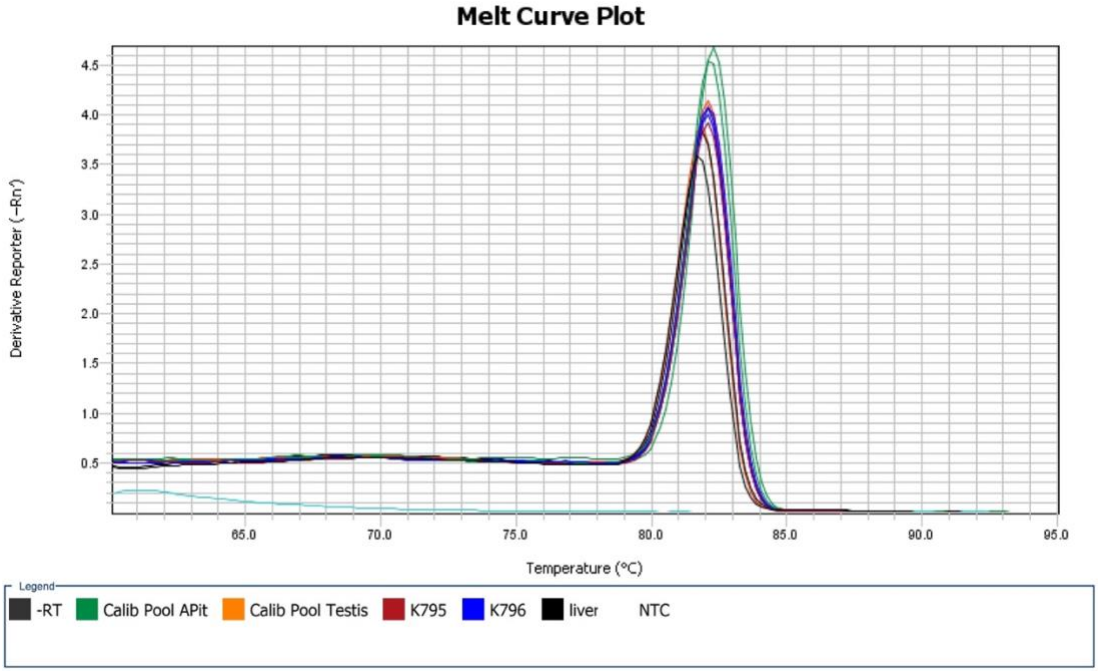

Figure C3a. The melting curve was generated during analysis of the expression of follicle stimulating hormone-beta (FSHβ) within the gestational day (GD) 53 caruncular tissue. The curve is generated at the end of each PCR run showing the specificity of amplification, which is evidenced by a single peak for each mRNA assay. The no template control (NTC) showed no peaks and the signal remained horizontal.

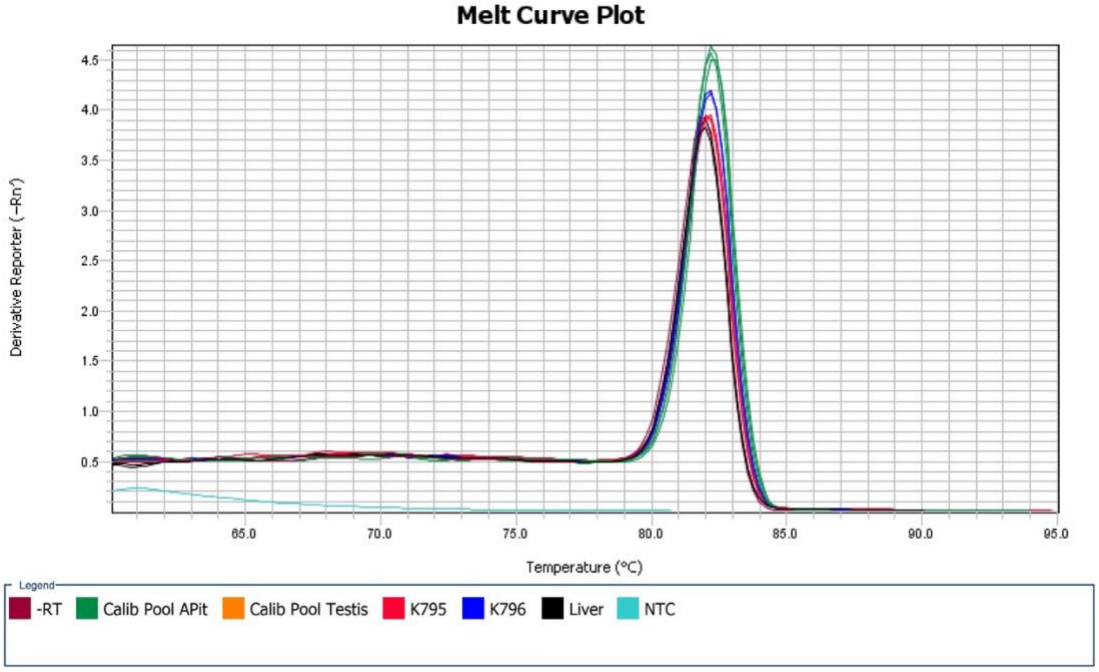

Figure C3b. The melting curve was generated during analysis of the expression of follicle stimulating hormone-beta (FSHβ) within the gestational day (GD) 53 cotyledonary tissue. The curve is generated at the end of each PCR run showing the specificity of amplification, which is evidenced by a single peak for each mRNA assay. The no template control (NTC) showed no peaks and the signal remained horizontal.

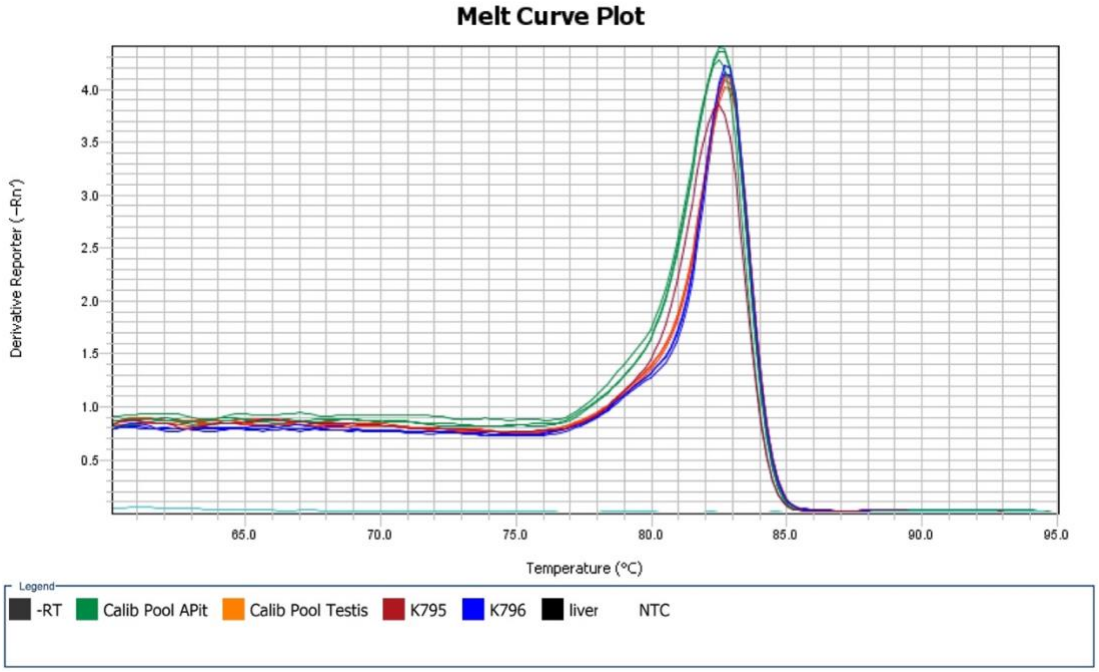

Figure C4a. The melting curve was generated during analysis of the expression of estrogen receptor alpha (ESR1) within the gestational day (GD) 53 caruncular tissue. The curve is generated at the end of each PCR run showing the specificity of amplification, which is evidenced by a single peak for each mRNA assay. The no template control (NTC) showed no peaks and the signal remained horizontal.

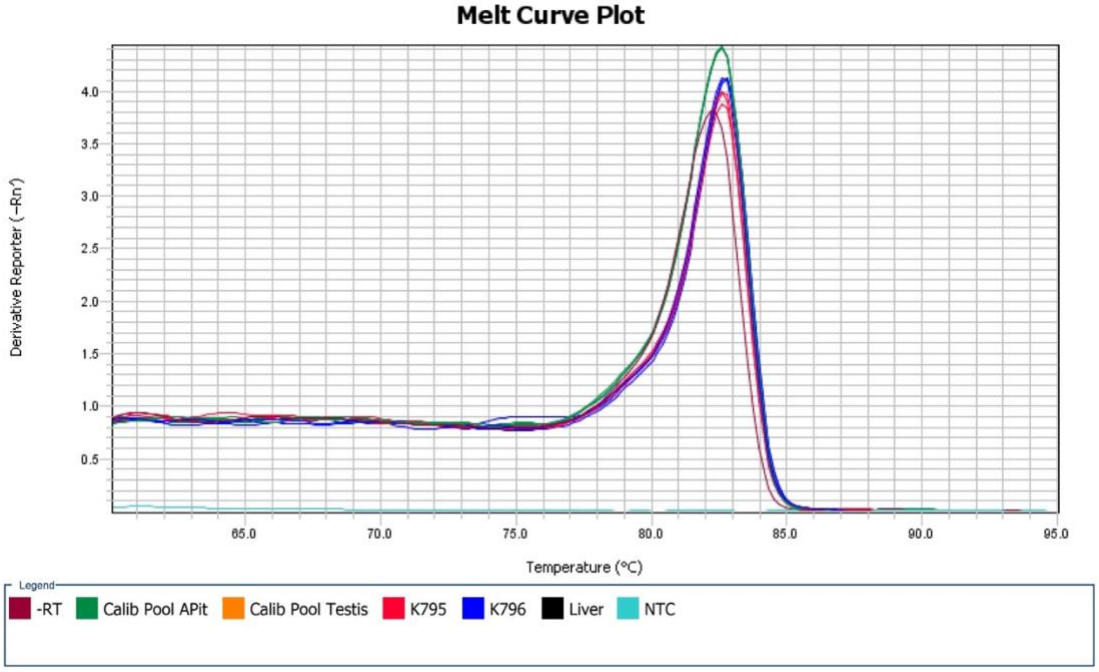

Figure C4b. The melting curve was generated during analysis of the expression of estrogen receptor alpha (ESR1) within the gestational day (GD) 53 cotyledonary tissue. The curve is generated at the end of each PCR run showing the specificity of amplification, which is evidenced by a single peak for each mRNA assay. The no template control (NTC) showed no peaks and the signal remained horizontal.

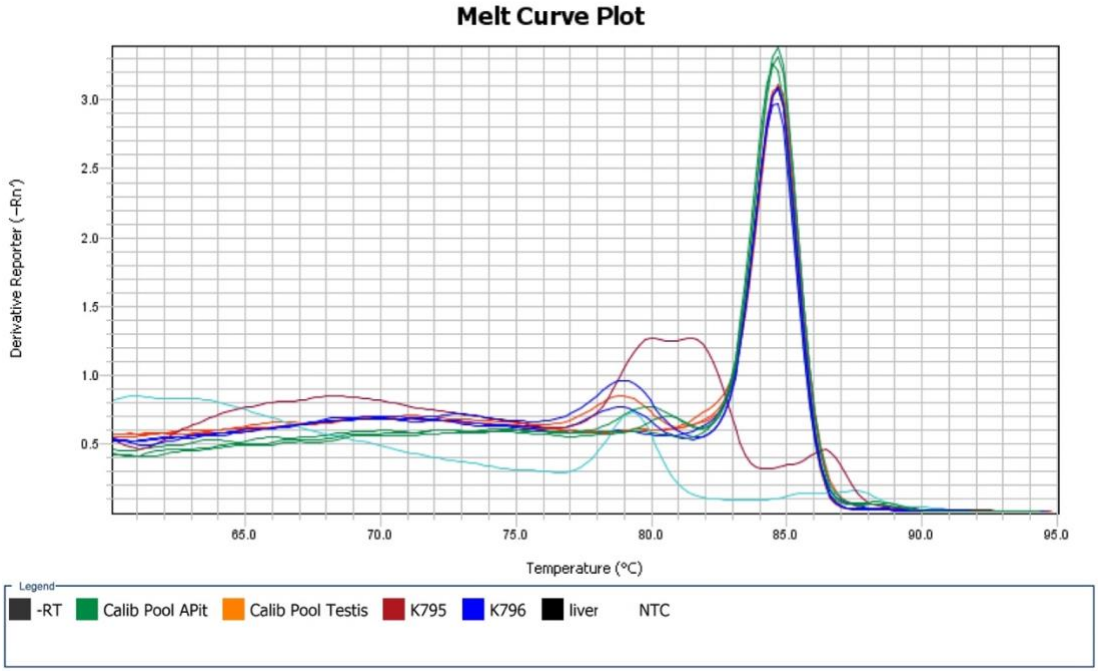

Figure C5a. The melting curve was generated during analysis of the expression of estrogen receptor beta (ESR2) within the gestational day (GD) 53 caruncular tissue. The curve is generated at the end of each PCR run showing the specificity of amplification, which is evidenced by a single peak for each mRNA assay. The no template control (NTC) showed no peaks and the signal remained horizontal.

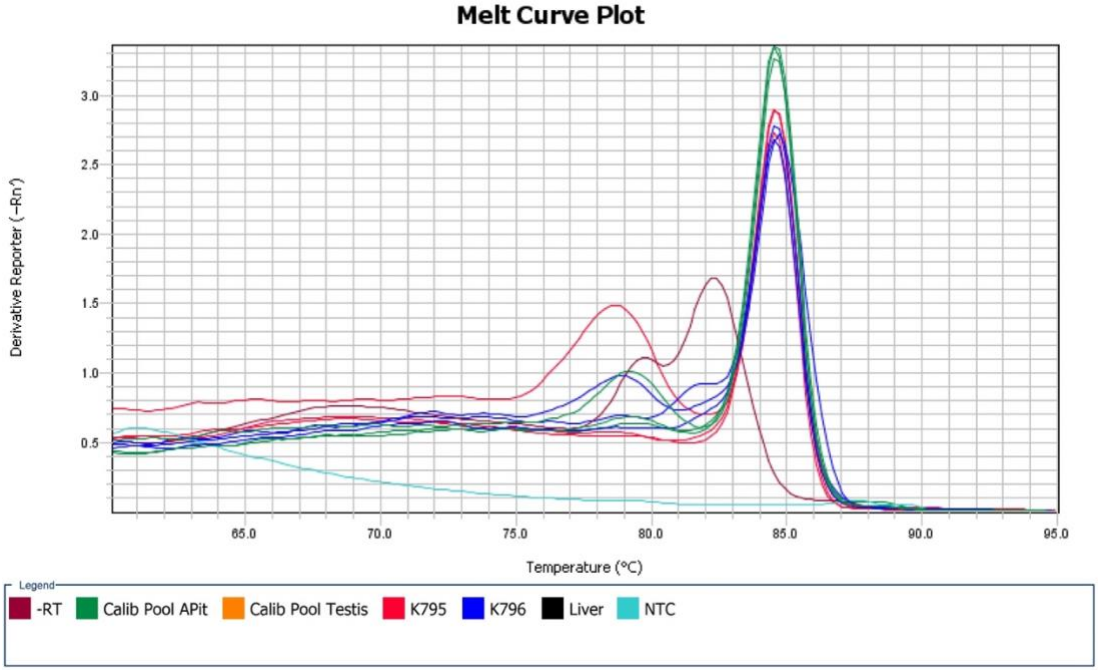

Figure C5b. The melting curve was generated during analysis of the expression of estrogen receptor beta (ESR) within the gestational day (GD) 53 cotyledonary tissue. The curve is generated at the end of each PCR run showing the specificity of amplification, which is evidenced by a single peak for each mRNA assay. The no template control (NTC) showed no peaks and the signal remained horizontal.

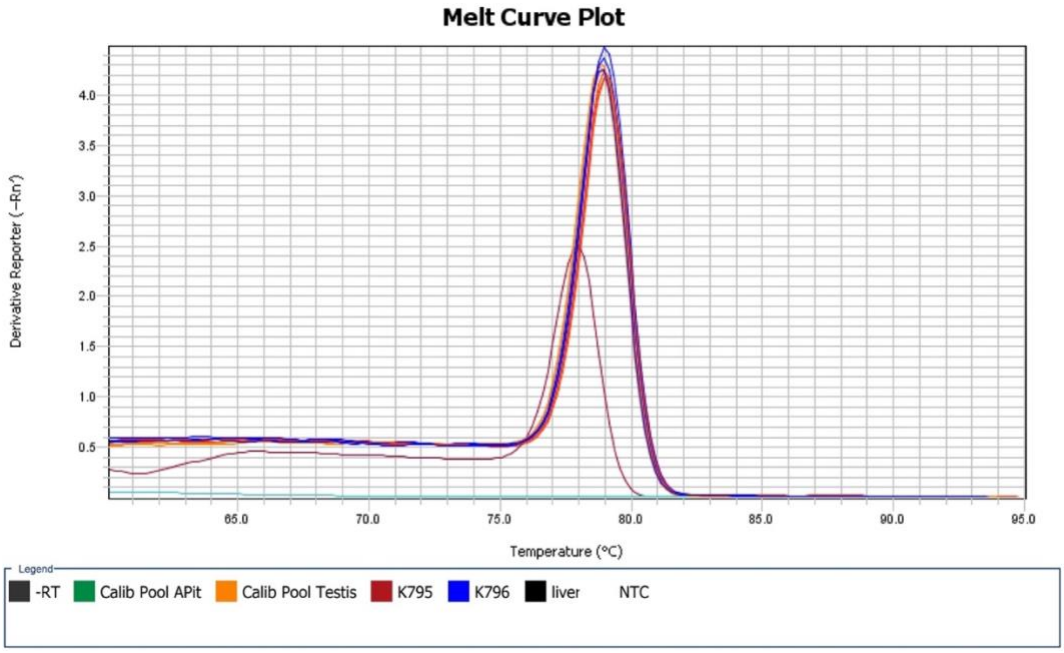

Figure C6a. The melting curve was generated during analysis of the expression of aromatase (CYP19) within the gestational day (GD) 53 caruncular tissue. The curve is generated at the end of each PCR run showing the specificity of amplification, which is evidenced by a single peak for each mRNA assay. The no template control (NTC) showed no peaks and the signal remained horizontal.

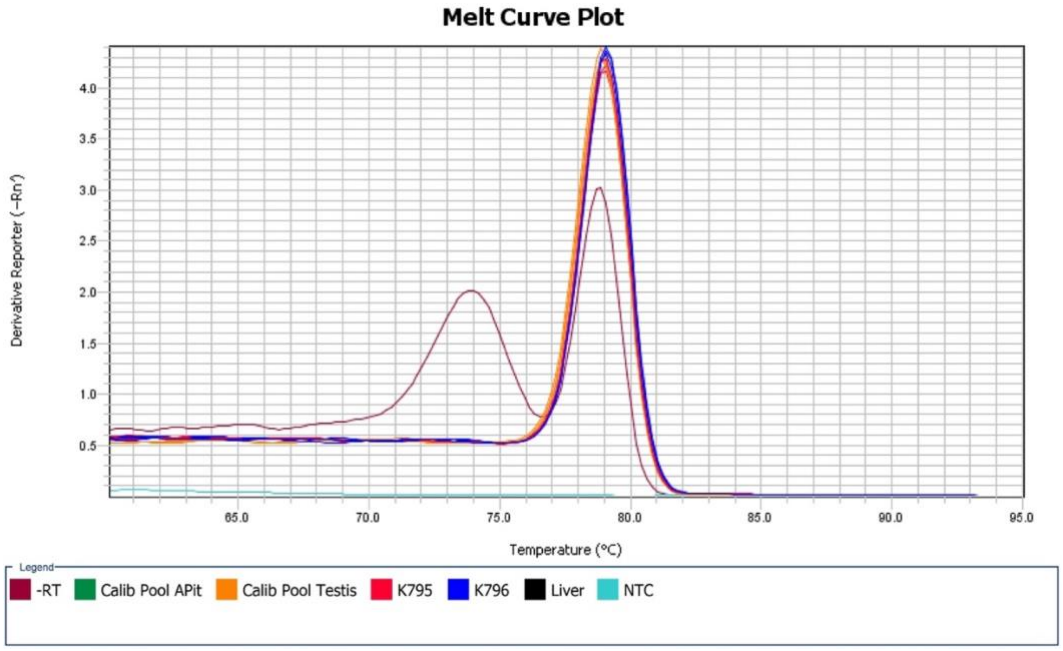

Figure C6b. The melting curve was generated during analysis of the expression of aromatase (CYP19) within the gestational day (GD) 53 cotyledonary tissue. The curve is generated at the end of each PCR run showing the specificity of amplification, which is evidenced by a single peak for each mRNA assay. The no template control (NTC) showed no peaks and the signal remained horizontal.

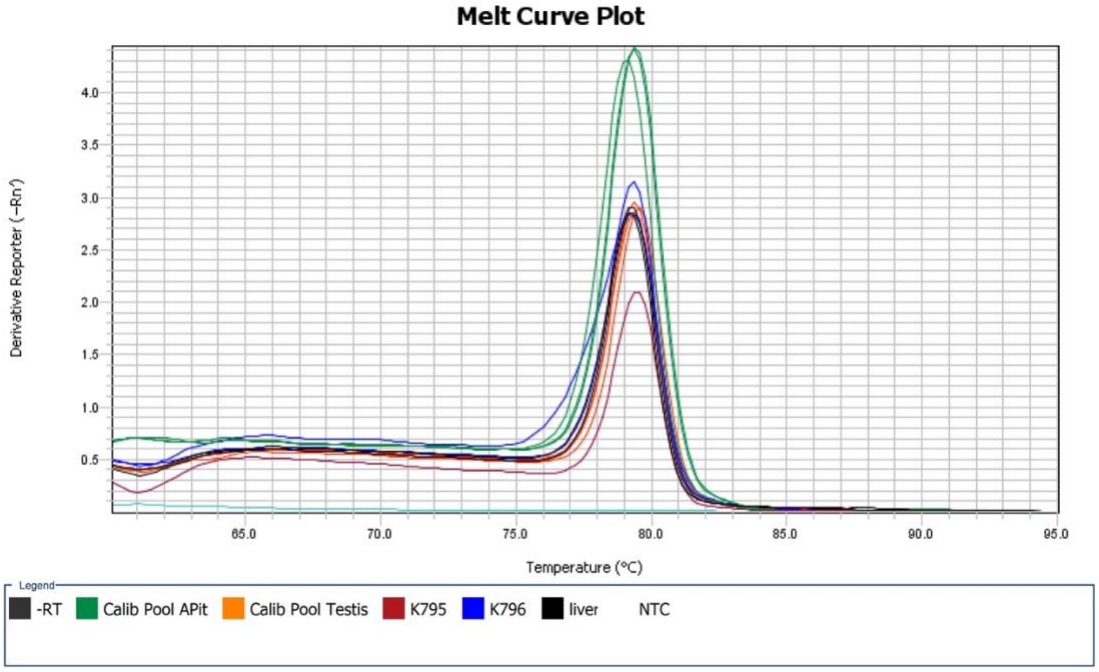

Figure C7a. The melting curve was generated during analysis of the expression of common alpha subunit (CAS) within the gestational day (GD) 53 caruncular tissue. The curve is generated at the end of each PCR run showing the specificity of amplification, which is evidenced by a single peak for each mRNA assay. The no template control (NTC) showed no peaks and the signal remained horizontal.

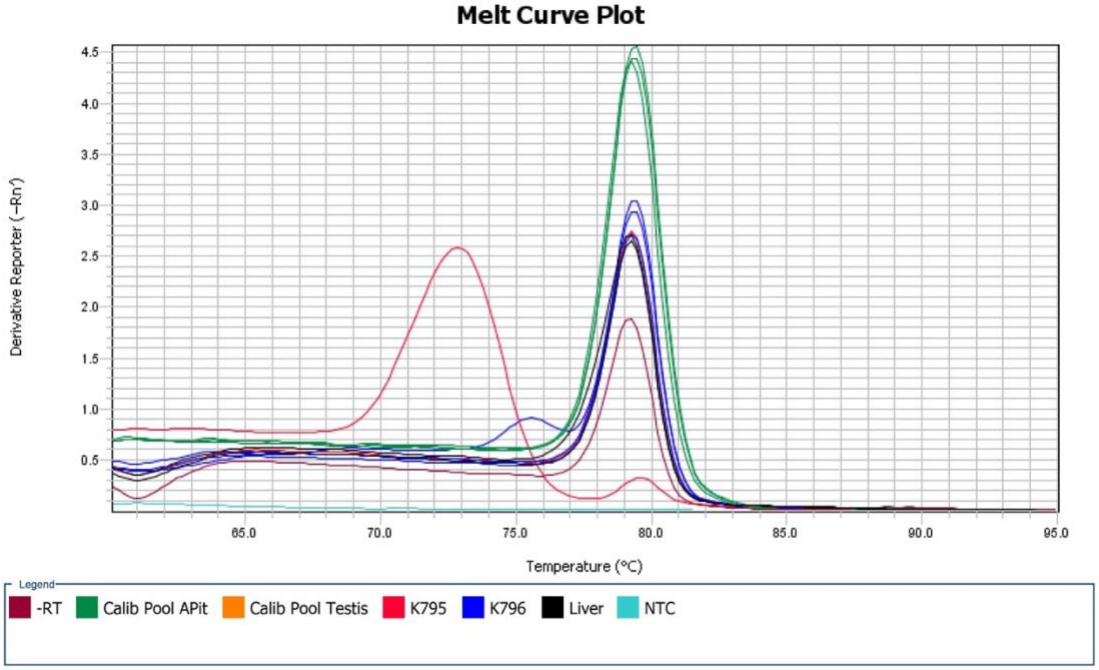

Figure C7b. The melting curve was generated during analysis of the expression of common alpha subunit (CAS) within the gestational day (GD) 53 cotyledonary tissue. The curve is generated at the end of each PCR run showing the specificity of amplification, which is evidenced by a single peak for each mRNA assay. The no template control (NTC) showed no peaks and the signal remained horizontal.

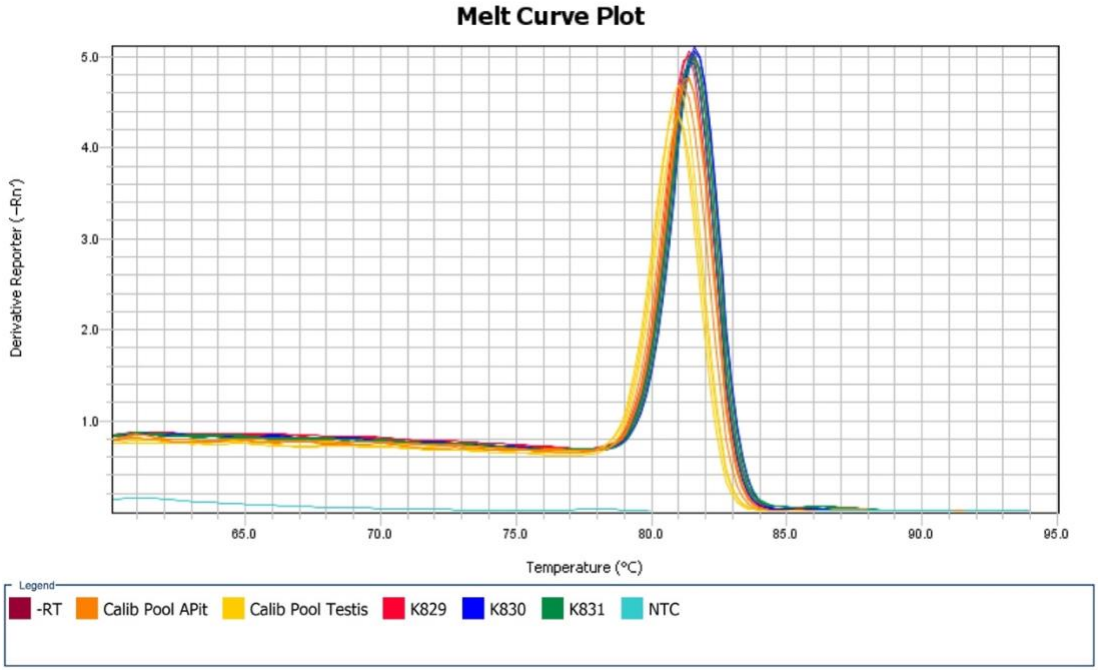

Figure C8a. The melting curve was generated during analysis of the expression of GAPDH within the gestational day (GD) 101 caruncular tissue. The curve is generated at the end of each PCR run showing the specificity of amplification, which is evidenced by a single peak for each mRNA assay. The no template control (NTC) showed no peaks and the signal remained horizontal.

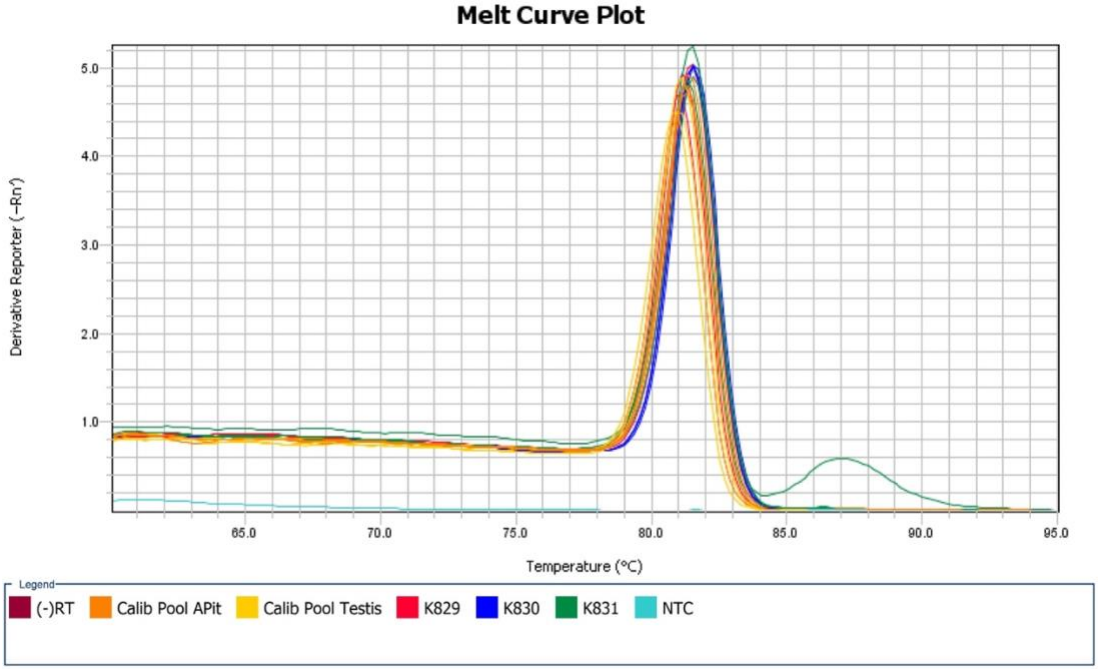

Figure C8b. The melting curve was generated during analysis of the expression of GAPDH within the gestational day (GD) 101 cotyledonary tissue. The curve is generated at the end of each PCR run showing the specificity of amplification, which is evidenced by a single peak for each mRNA assay. The no template control (NTC) showed no peaks and the signal remained horizontal.

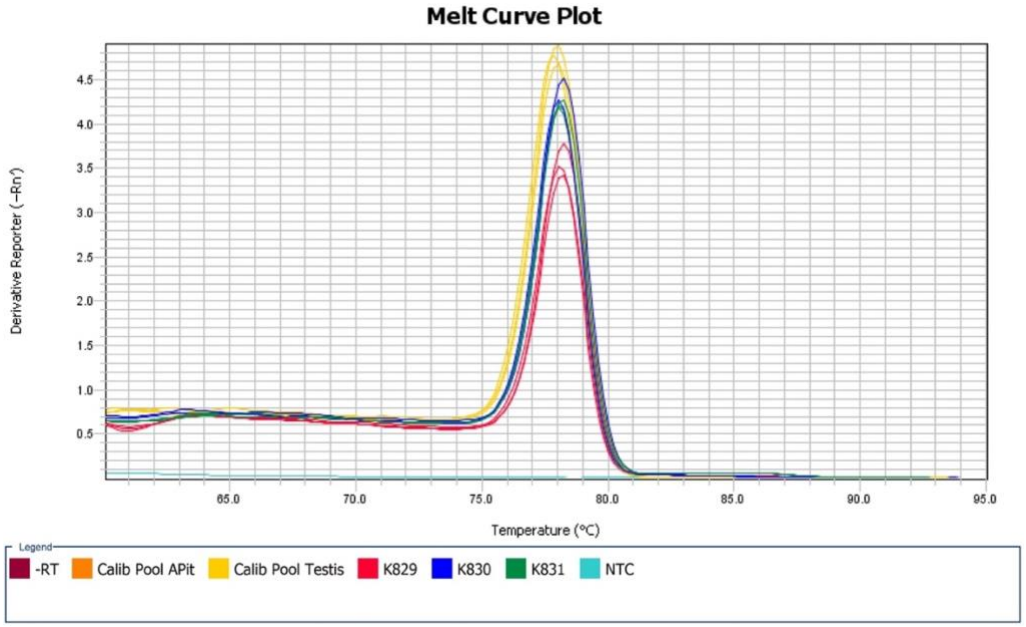

Figure C9a. The melting curve was generated during analysis of the expression of follicle stimulating hormone receptor (FSHR) within the gestational day (GD) 101 caruncular tissue. The curve is generated at the end of each PCR run showing the specificity of amplification, which is evidenced by a single peak for each mRNA assay. The no template control (NTC) showed no peaks and the signal remained horizontal.

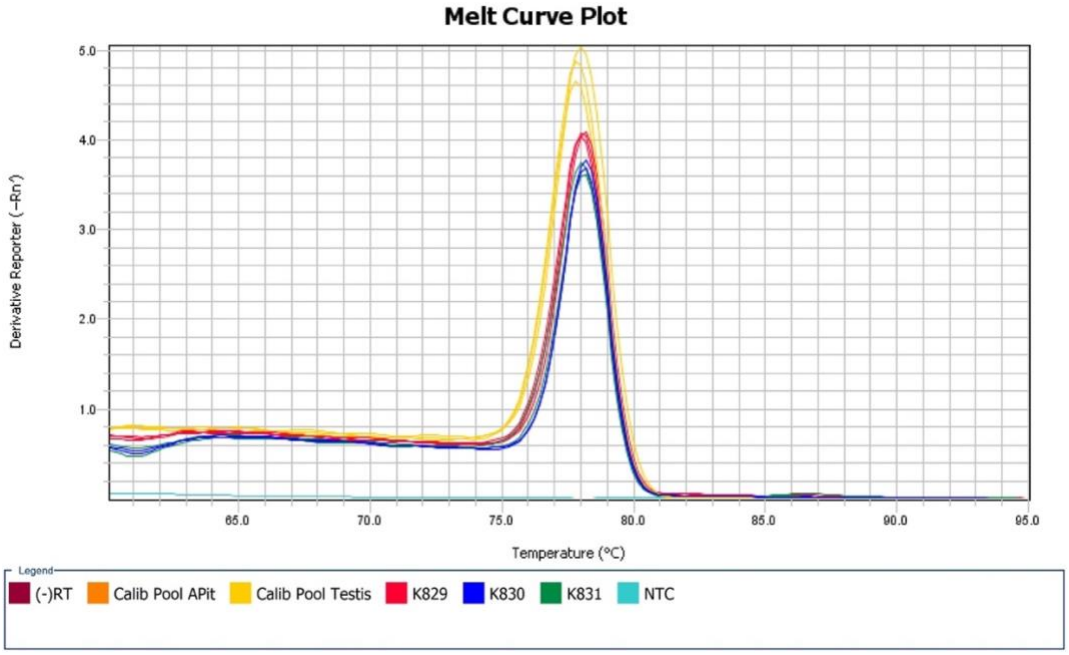

Figure C9b. The melting curve was generated during analysis of the expression of follicle stimulating hormone receptor (FSHR) within the gestational day (GD) 101 cotyledonary tissue. The curve is generated at the end of each PCR run showing the specificity of amplification, which is evidenced by a single peak for each mRNA assay. The no template control (NTC) showed no peaks and the signal remained horizontal.

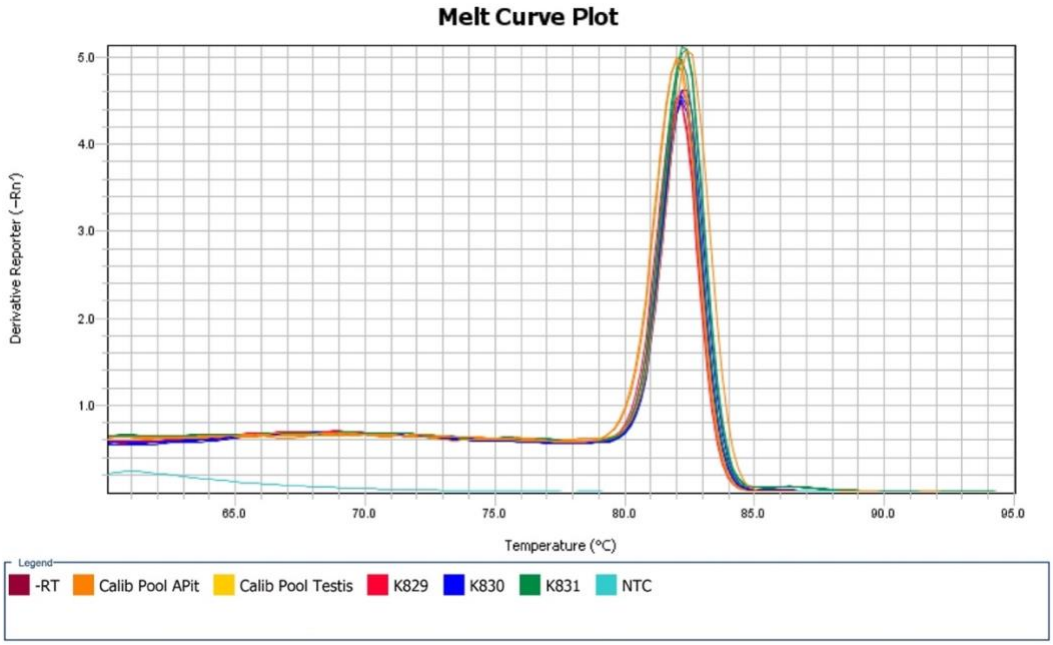

Figure C10a. The melting curve was generated during analysis of the expression of follicle stimulating hormone-beta (FSHβ) within the gestational day (GD) 101 caruncular tissue. The curve is generated at the end of each PCR run showing the specificity of amplification, which is evidenced by a single peak for each mRNA assay. The no template control (NTC) showed no peaks and the signal remained horizontal.

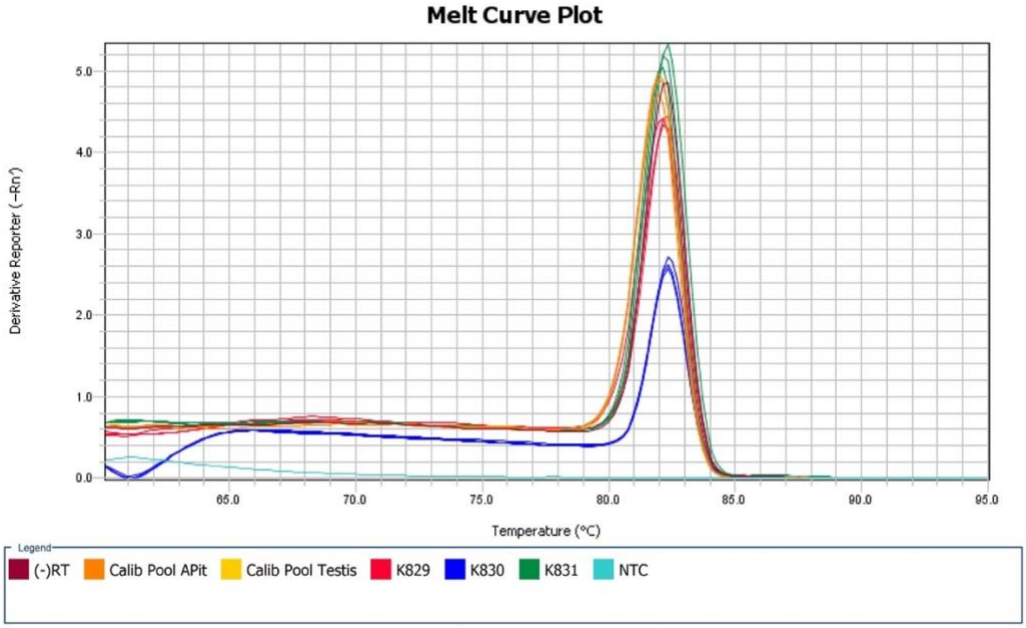

Figure C10b. The melting curve was generated during analysis of the expression of follicle stimulating hormone receptor-beta (FSHβ) within the gestational day (GD) 101 cotyledonary tissue. The curve is generated at the end of each PCR run showing the specificity of amplification, which is evidenced by a single peak for each mRNA assay. The no template control (NTC) showed no peaks and the signal remained horizontal.

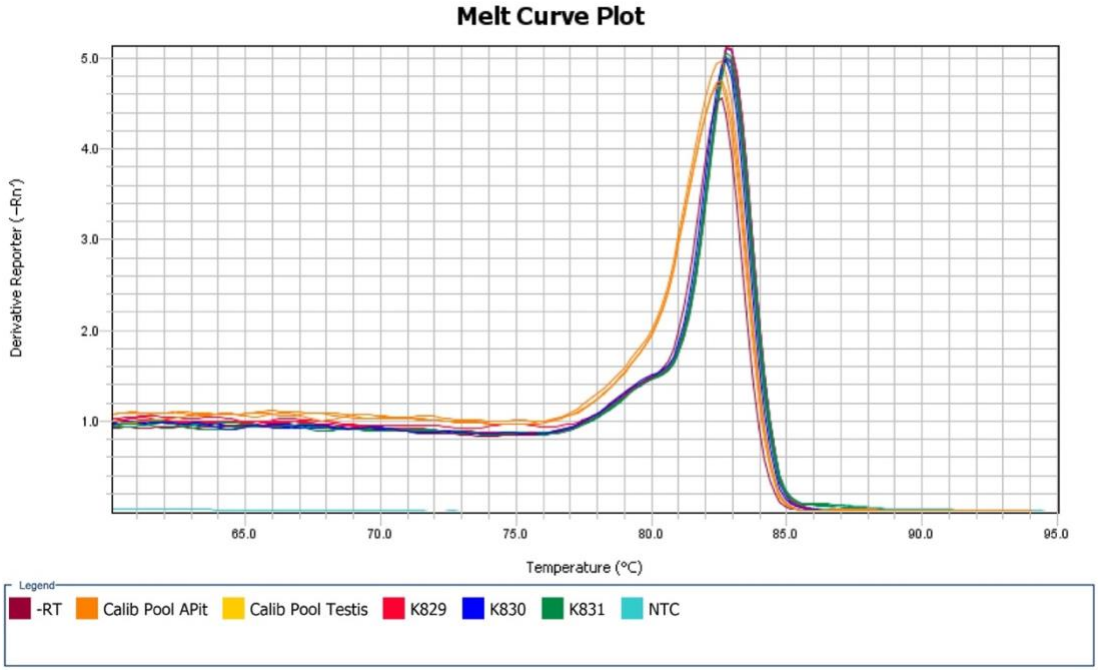

Figure C11a. The melting curve was generated during analysis of the expression of estrogen receptor alpha (ESR1) within the gestational day (GD) 101 caruncular tissue. The curve is generated at the end of each PCR run showing the specificity of amplification, which is evidenced by a single peak for each mRNA assay. The no template control (NTC) showed no peaks and the signal remained horizontal.

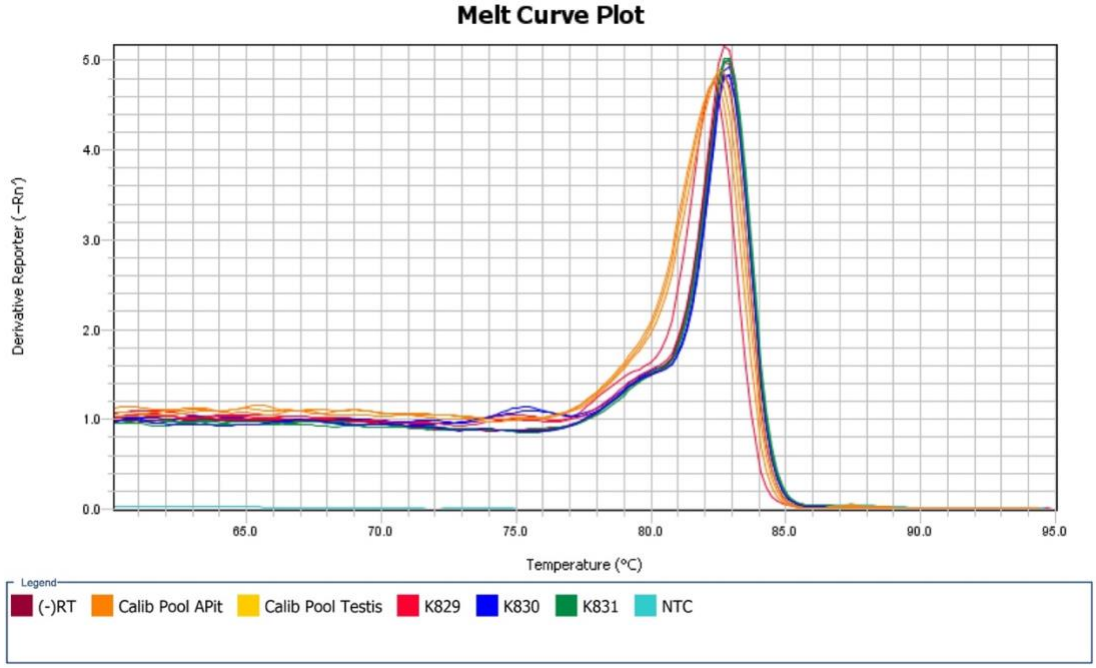

Figure C1lb. The melting curve was generated during analysis of the expression of estrogen receptor alpha (ESR1) within the gestational day (GD) 101 cotyledonary tissue. The curve is generated at the end of each PCR run showing the specificity of amplification, which is evidenced by a single peak for each mRNA assay. The no template control (NTC) showed no peaks and the signal remained horizontal.

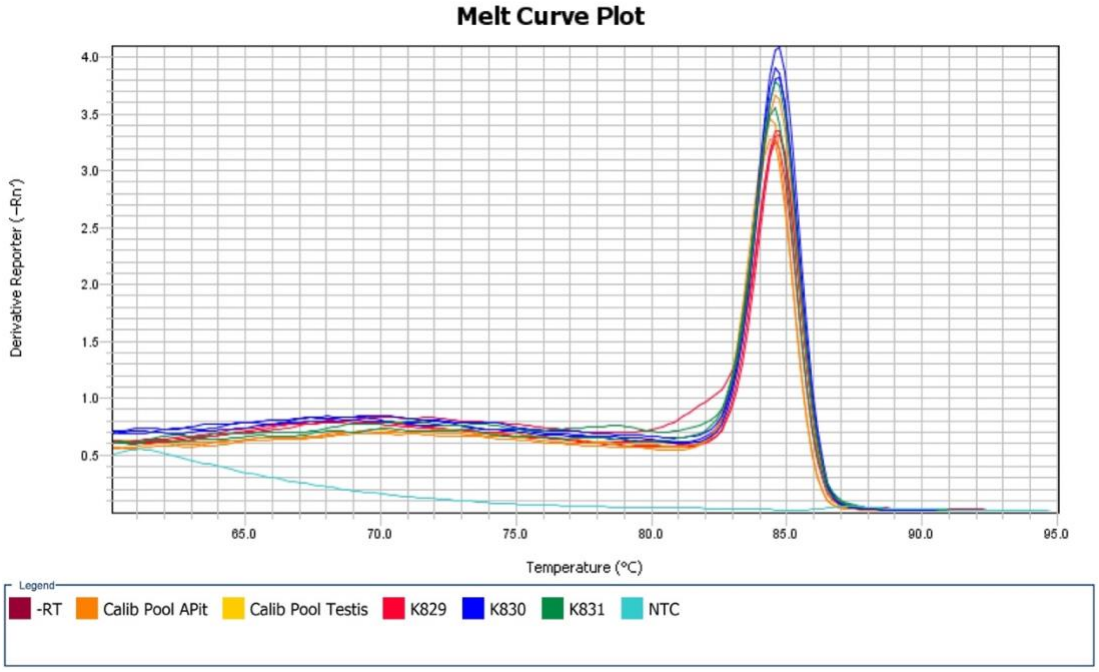

Figure C12a. The melting curve was generated during analysis of the expression of estrogen receptor beta (ESR2) within the gestational day (GD) 101 caruncular tissue. The curve is generated at the end of each PCR run showing the specificity of amplification, which is evidenced by a single peak for each mRNA assay. The no template control (NTC) showed no peaks and the signal remained horizontal.

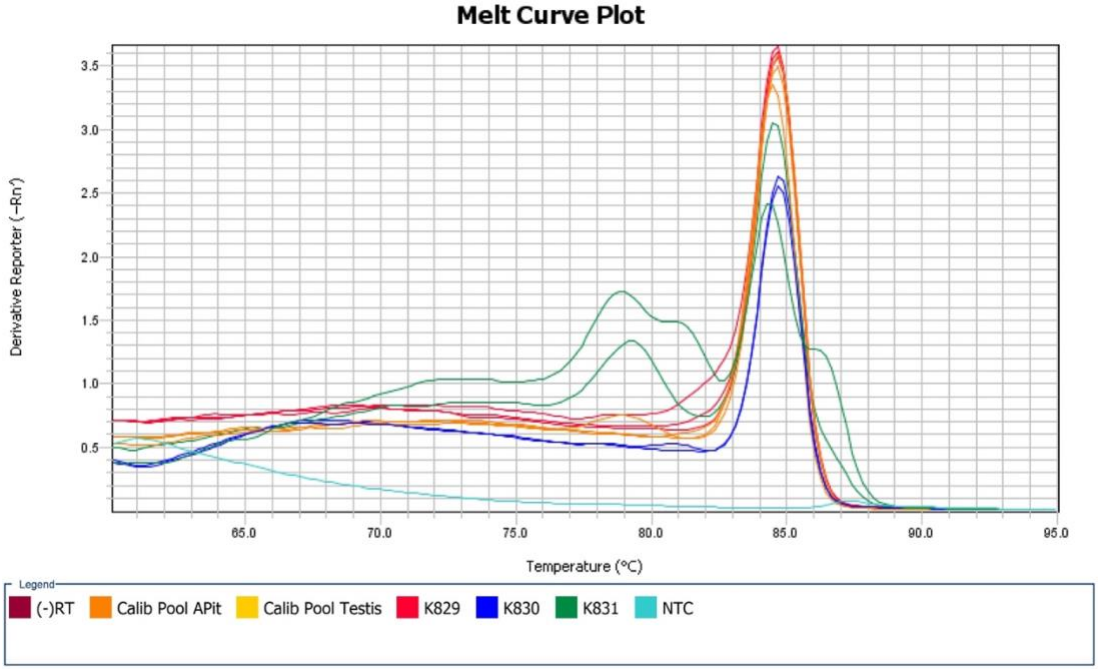

Figure C12b. The melting curve was generated during analysis of the expression of estrogen receptor beta (ESR2) within the gestational day (GD) 101 cotyledonary tissue. The curve is generated at the end of each PCR run showing the specificity of amplification, which is evidenced by a single peak for each mRNA assay. The no template control (NTC) showed no peaks and the signal remained horizontal.

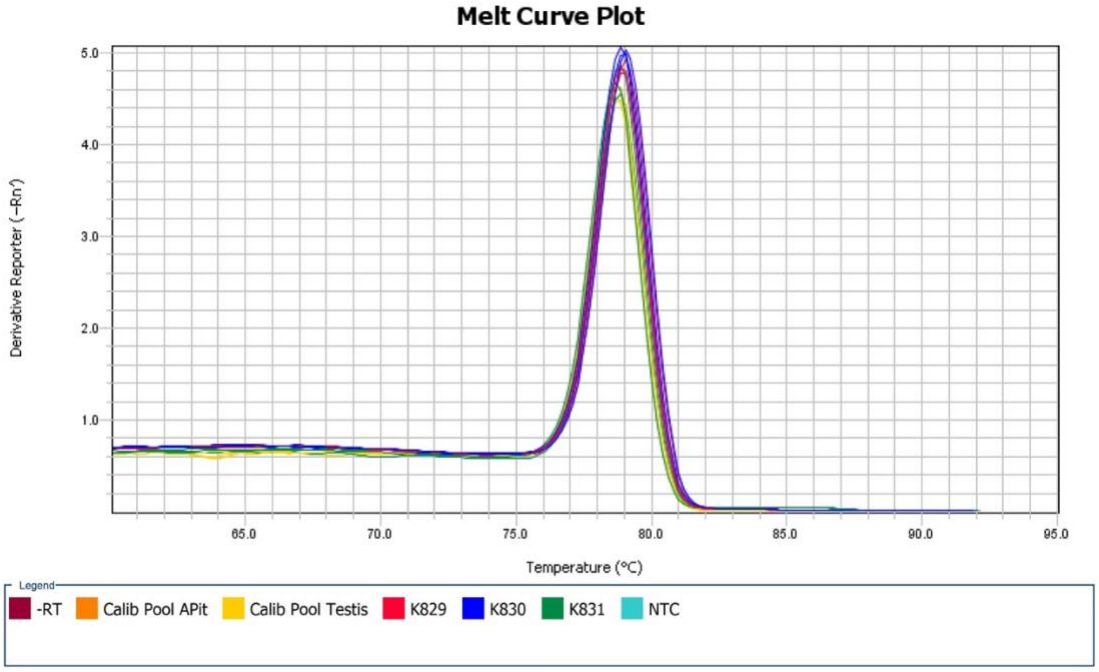

Figure C13a. The melting curve was generated during analysis of the expression of aromatase (CYP19) within the gestational day (GD) 101 caruncular tissue. It is generated at the end of each PCR run showing the specificity of amplification, which is evidenced by a single peak for each mRNA assay. The no template control (NTC) showed no peaks and the signal remained horizontal.

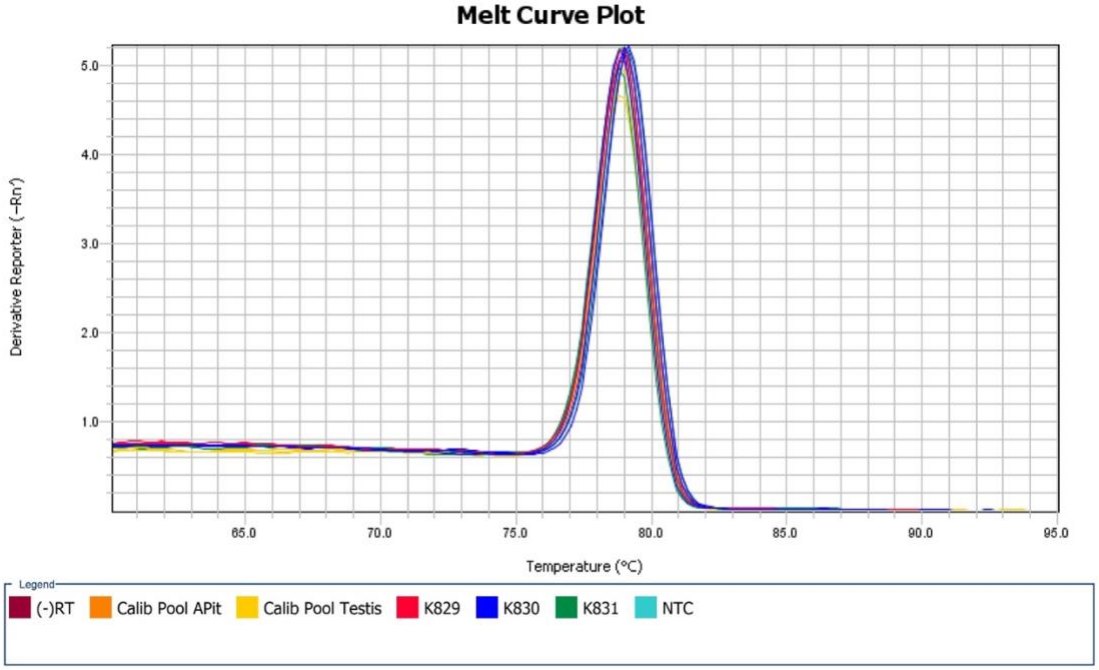

Figure C13b. The melting curve was generated during analysis of the expression of aromatase (CYP19) within the gestational day (GD) 101 cotyledonary tissue. The curve is generated at the end of each PCR run showing the specificity of amplification, which is evidenced by a single peak for each mRNA assay. The no template control (NTC) showed no peaks and the signal remained horizontal.

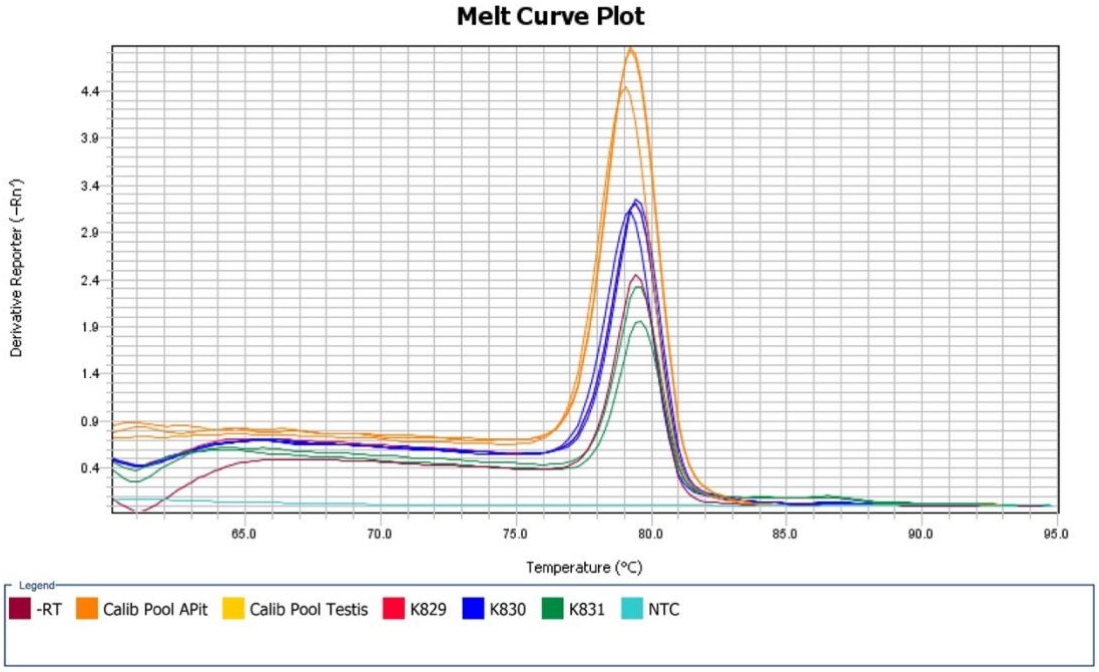

Figure C14a. The melting curve was generated during analysis of the expression of common alpha subunit (CAS) within the gestational day (GD) 101 caruncular tissue. The curve is generated at the end of each PCR run showing the specificity of amplification, which is evidenced by a single peak for each mRNA assay. The no template control (NTC) showed no peaks and the signal remained horizontal.

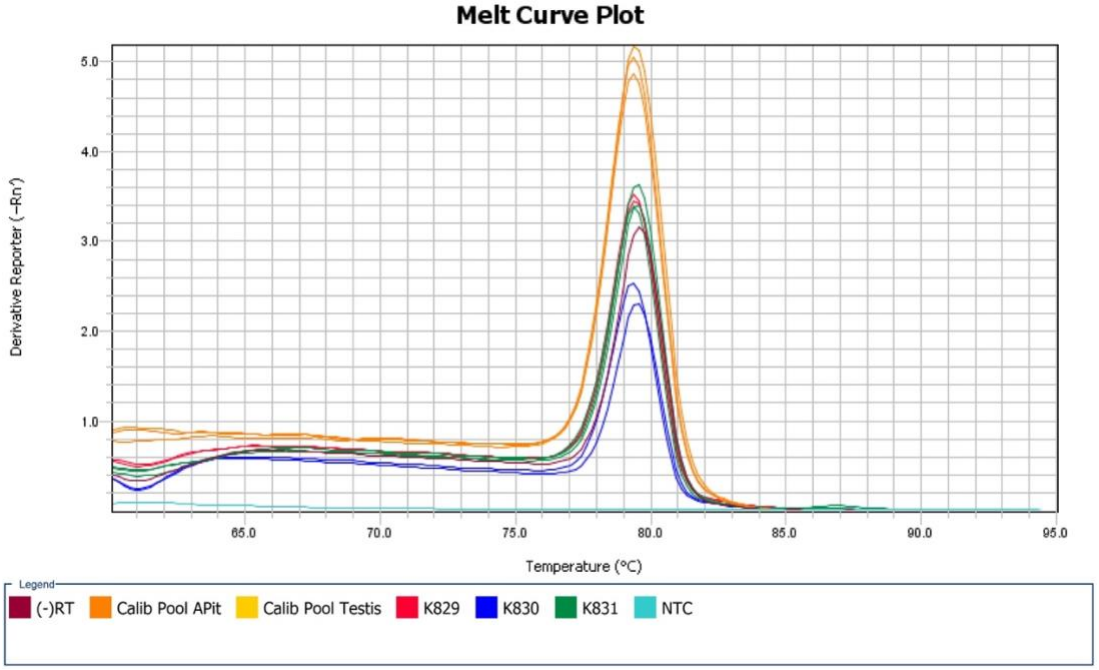

Figure C14b. The melting curve was generated during analysis of the expression of common alpha subunit (CAS) within the gestational day (GD) 101 cotyledonary tissue. The curve is generated at the end of each PCR run showing the specificity of amplification, which is evidenced by a single peak for each mRNA assay. The no template control (NTC) showed no peaks and the signal remained horizontal.

APPENDIX D: PRELIMINARY DATA

D.1 Preliminary gel electrophoresis confirming product was likely present in desired samples.

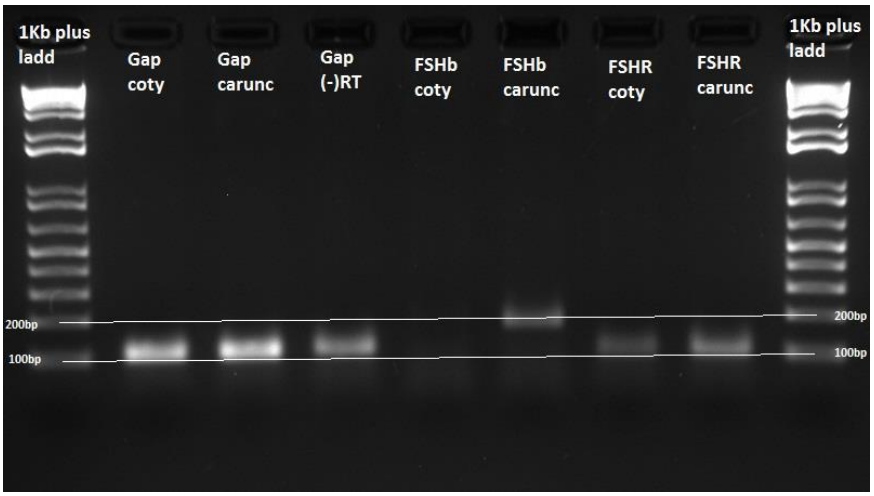

Figure D1. An ethidium bromide agarose gel electrophoresis (2% agarose) of RT-PCR amplified products using species-specific PCR primer sets. The lane on the far left and right are the 1kb DNA ladder. Caruncular and cotyledonary tissues from GD 101 was evaluated with GAPDH, follicle stimulating hormone-beta (FSHβ) and follicle stimulating hormone receptor (FSHR) primers. GAPDH product size is 107 base pairs, FSHβ product size is 175 base pairs, FSHR product size is 99 base pairs.

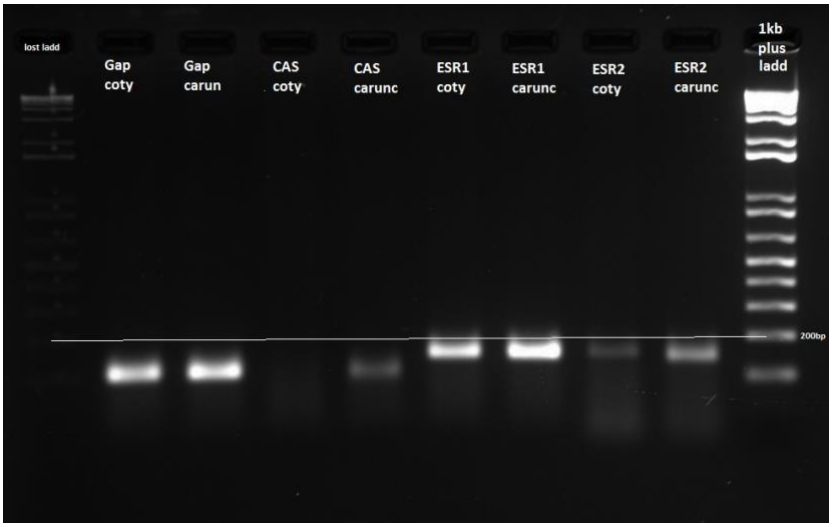

Figure D2. An ethidium bromide agarose gel electrophoresis (2% agarose) of RT-PCR amplified products using species-specific PCR primer sets. The lane on the far left and right are the 1kb DNA ladder. Caruncular and cotyledonary tissues from GD 101 evaluated with GAPDH, common alpha subunit (CAS), estrogen receptor alpha (ESR1) and estrogen receptor alpha (ESR2) primers. GapDH product size is 107 base pairs, CAS product size is 93 base pairs, ESR1 product size is 146 base pairs and ESR2 product size is 140 base pairs.

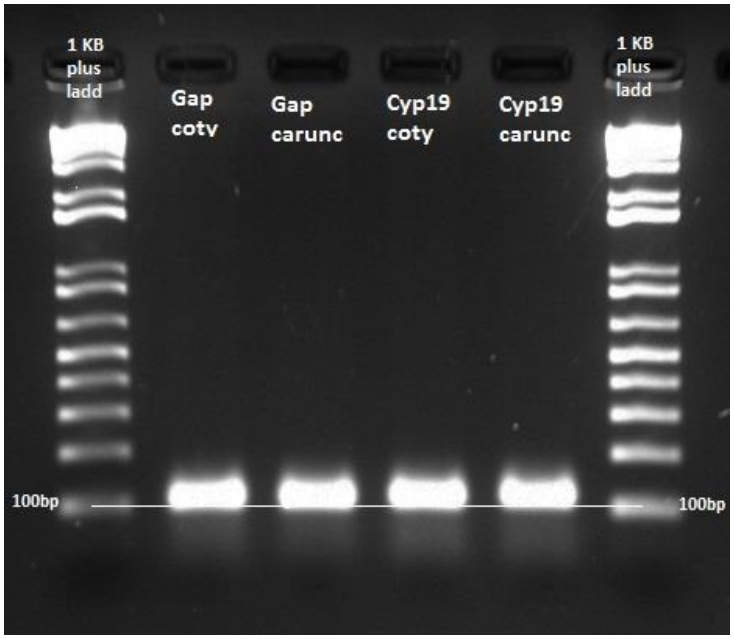

Figure D3. An ethidium bromide agarose gel electrophoresis (2% agarose) of RT-PCR amplified products using species-specific PCR primer sets. The lane on the far left and right are the 1kb DNA ladder. Caruncular and cotyledonary tissues from GD 101 evaluated with GAPDH and aromatase (CYP19) primers. GAPDH product size is 107 base pairs, and CYP19 product size is 110 base pair.

D2. Bovine FSHβ Primer Validation

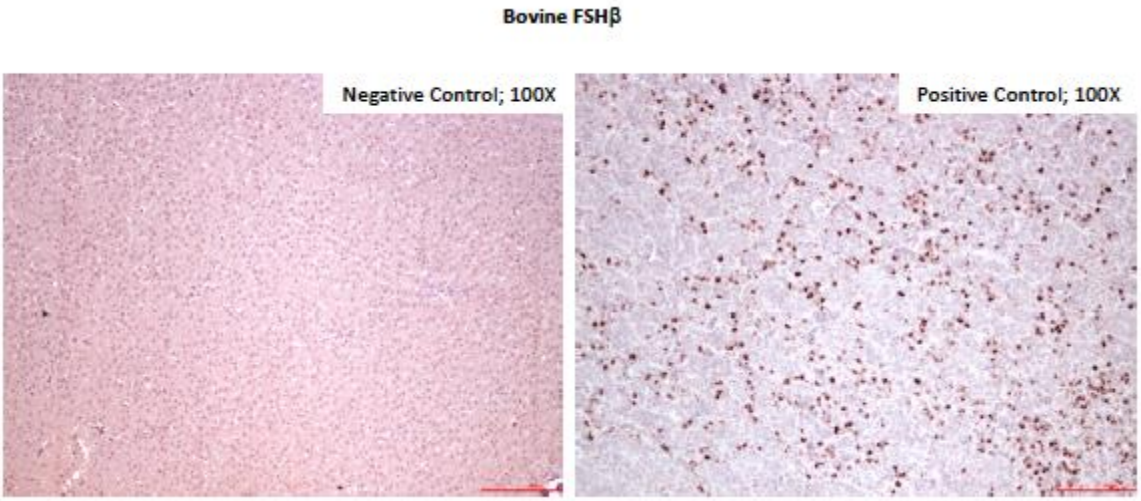

Figure D4. Preliminary immunohistochemistry data for validation of follicle stimulating hormone-beta (FSHβ) primer. The negative control (bovine liver) showed no immunoexpression (original magnification 10X, left) and the positive control (bovine maternal anterior pituitary) showed marked immunoexpression (original magnification 10X, right).

APPENDIX E: TABLE OF ABBREVIATIONS

Table of Abbreviations	
Abbreviation	**Description**
3β-HSD	3β - hydroxysteroid dehydrogenase
BGC	Binucleate giant cell
CAS	Common alpha subunit
CL	Corpus luteum
CYP19	Aromatase
ESR1	Estrogen receptor alpha
ESR2	Estrogen receptor beta
FSHβ	Follicle stimulating hormone (β subunit)
FSHR	Follicle stimulating hormone receptor
GapDH	Glyceraldehyde 3-phosphate dehydrogenase
GD	Gestational day
GH	Growth hormone
GnRH	Gonadotropin releasing hormone
IHC	Immunohistochemistry
Kiss1	Kisspeptin
LE	Luminal epithelium
LH	Luteinizing hormone
MRP	Maternal recognition of pregnancy
MRT	Minus reverse transcriptase
NTC	Non-template control
oIFN-tau	Interferon-tau
OXT	Oxytocin
OXTR	Oxytocin receptor
PGE	Prostaglandin E
$PGF_{2\alpha}$	Prostaglandin $F_{2\alpha}$

APPENDIX E: TABLE OF ABBREVIATIONS (Continued)

PGR	Progesterone receptor
PKA	Protein kinase A
PL	Placental lactogen
PTGS2	Prostaglandin synthase 2
PSPB	Pregnancy specific protein B
RFRP-3	RFamide-related peptide 3
RIA	Radioimmunoassay
RT-PCR	Real-time polymerase chain reaction
sGE	Superficial ductal glandular epithelium
StAR	Steroidogenic acute regulatory protein